Applied and Computational Mathematics
2024; 13(1): 8-28
http://www.sciencepublishinggroup.com/j/acm
doi: 10.11648/j.acm.20241301.12
ISSN: 2328-5605 (Print); ISSN: 2328-5613 (Online)

Soret and Dufour Effects on MHD Fluid Flow Through a Collapssible Tube Using Spectral Based Collocation Method

Victor Kaigalula[1, *], Samuel Mutua[2]

[1]Department of Mathematics, Pan African University Institute for Basic Sciences, Innovation and Technology, Nairobi, Kenya
[2]Mathematics, Statistics and Physical Sciences Department, Taita Taveta University, Nairobi, Kenya

Email address:

kaigalula119@gmail.com (Victor Kaigalula), felexmutua@gmail.com (Samuel Mutua)
[*]Corresponding author

To cite this article:

Victor Kaigalula, Samuel Mutua. Soret and Dufour Effects on MHD Fluid Flow Through a Collapssible Tube Using Spectral Based Collocation Method. *Applied and Computational Mathematics, 13*(1), 8-28. https://doi.org/10.11648/j.acm.20241301.12

Received: December 21, 2023; **Accepted:** January 8, 2024; **Published:** February 28, 2024

Abstract: This paper examine numerical study for soret and dufour effects on unsteady Newtonian MHD fluid flow with mass and heat transfer in a collapsible elastic tube using Spectral Collocation technique. The objective of the study is to determine the velocity, temperature and concentration profiles together with heat and mass transfer rates. The governing equations are continuity, momentum, energy and concentration equation. The system of nonlinear partial differential equations governing the flow solved numerically by applying collocation method and implemented in MATLAB. The numerical solution of the profiles displayed both by graphically and numerically for different values of the physical parameters. The effects of varying various parameters such as Reynolds number, Hartmann number, Soret number, Dufour number and Prandtl number on velocity, temperature and concentration profiles also the rates of heat and mass transfer are discussed. The findings of this study are important due to its wide range of application including but not limited to medical fields, biological sciences and other physical sciences where collapsible tubes are applied.

Keywords: Collapsible Tube, MHD, Soret-Dufour, Numerical Technique, Spectral Collocation

1. Introduction

Fluid flow through a collapsible elastic tubes has been studied by a number of researchers due to its wide and varied applications in different areas in real life. Collapsible tubes are tubes with circular cross-section which are able to accommodate elastically deformation when exposed to internal-external pressure variations. This tubes are very important in our daily life due to it involves in different areas such as in biological studies, veins, arteries, urethra and airways tubes are examples of collapsible elastic tube. This study of MHD fluid flow through collapsible tube with mass and heat transfer is of utmost importance due to its application in physical and natural sciences and engineering. The experimental and theoretical research on unsteady incompressible MHD flows is important to scientific and engineering fields in particular biological flows such as blood flow in arteries or veins, flow of urine in urethra and air flow in the bronchial airways. Also can be used to study and prediction of many diseases such as the lung disease (asthma and emphysema), or cardiovascular diseases (heart stroke). It is also has importance in engineering processes such as in MHD pumps, MHD power generators for electricity production, accelerators, MHD flow meters, electrostatic filters, the design of cooling systems with liquid metals, and in geothermal power stations.

In the human body, capillary tubes such as blood vessels, urethra, bronchioles, and ureters play important roles in the transport of fluids. Blood is essential in sustaining life as it transport oxygen and nutrients to all parts of the body, relays chemical signals and moves metabolic wastes to the kidney for elimination. Similarly in the industries collapse may be experienced during cementing operations, trapped fluid expansion or well evaculation. A quantitative models of fluid flows are important, to date numerous mathematical models have been developed describing MHD fluid flow in different areas but few have done in collapsible tube.

Makinde investigated mathematical model which describing fluid dynamics in a collapsible tube, he constructed analytical solution for problem using pertubation technique and Hermite-Pade approximations [1]. Luo analyzes the unsteady behavior and linear stability of the flow in a Collapsible tube by using a fluid beam model [2]. Lakshmi Narayana established Soret and Dufour effects on free convection heat and mass transfer from horizontal flat plate in a Darcy porous medium [3]. Odejide examined an incompressible viscous fluid flow and heat transfer in a collapsible tube [4]. Cheng analyze Soret and Dufour effects on natural convection heat and mass transfer from a vertical cone in a porous medium [5]. Emilie investigated an accurate modeling of unsteady flows in collapsible tubes. One-dimensional Runge-Kutta discontinuous Galerkin method coupled with lumped parameter models for the boundary conditions was used [6]. El-Kabeir studied soret and dufour effects on heat and mass transfer due to a stretching cylinder saturated porous medium which chemically reactive species [7]. Dulal examined combined effects of Soret (thermal-diffusion) and Dufour (diffusion-thermo) on a mixed convection over a stretching sheet embedded in a saturated porous medium in the presence of thermal radiation and chemical reaction studied. He found that temperature profiles increase with increase in Dufour number [8]. Chatterjee investigate Soret and dufour effects on MHD convective heat and mass transfer of a power-law fluid over an inclined plate with variable thermal conductivity in a porus medium. Nonlinear ordinary differential equations are solved numerically based on shooting method with Runge-Kutta Fehlberg integration scheme [9]. Siviglia established multiple states for flow through a Collapsible tube with discontinuities. It was established that the complexity of the fluid-structure gives Collapsible tubes their specific dynamic features. The numerical solution was obtained by using finite volume method of the path conservative type [10].

Kanyiri studied the effects of flow parameters (tube stiffiness and longitudinal tension) on the flow variables of a Newtonian, steady incompressible fluid flowing through cylindrical collapsible tube. The result show that the flow parameter considered are directly proportional to both the cross sectional area and internal pressure and inversely proportional to the flow velocity [11]. Ullah investigate a study of two dimensional unsteady MHD free convection flow over a vertical plate in the presence of radiation. They examine radiactive effects on the MHD free convection flow of an electrically conducting incompressible viscous fluid over a vertical plate. Dimensionless momentum and energy equations were solved numerically by using explicit finite difference method. It was established that velocity profiles decreases with an increasing Grashof number. Also there was decline of velocity profiles because of increasing values of Eckert number as a result heat transfer of the flow reduced the driving force to the kinetic energy [12]. Kaigalula investigate fluid flow through a collapsible elastic tube, it is observed that increase in soret effects causes concentration distributions to increase [13]. Inyang examine heat transfer of helical coil in heat exchangers (HCHE). It demonstrated that the helical heat exchanger provide more excellent heat transfer performance and effectiveness than straight tubes. It was obtained that heat transfer coefficient increased with an increase in curvature ratio of HCHE fot the same flow rates [14]. [15] in this study, an incompressible viscous fluid flow and heat transfer in a collapsible tube with heat source or sink is examined. Mwangi described unsteady MHD fluid flow in a collapsible tube. The fluid was considered to be Newtonian. The non linear partial differential equations which were solved numerically using finite difference method (FDM) [16]. Anand investigated steady low Reynolds number flow of a generalized Newtonian fluid through a slender elastic tube [17]. Mehdari investigated analytical modelling of an unsteady fluid flow through an elastic tube. The fluid was considered to be Newtonian and Incompressible, they took into consideration large Reynolds number and a small aspect ratio, the tube was assumed to be having a small shell, which they considered to be the source of asymmetric vibration [18]. Maurice examine unsteady flow of Newtonian fluid in collapsible tube. They formulated a mathematical model of a Newtonian fluid in a collapsible tube to simulate physiological flows such as flow of blood and urine within human body system [19]. Chepkonga investigated fluid flow coupled with heat transfer through a vertical cylindrical collapsible tube in the presence of magnetic field and an obstacle [20]. Alsemiry investigated numerical solution of blood flow and mass transport in an elastic tube with multiple stenosis [21]. Idowu investigate effects of thermophoresis, Soret-Dufour on heat and mass transfer flow of magnetohydrodynamics non-Newtonian nanofluid over an inclined plate [22]. Priyadharsin studied the unsteady flow of collapsible tube under transverse magneto hydrodynamic fluid. Their aim was to determine the velocity and temperature profiles, and the effects of some non-dimensional numbers of the taken nanofluid. [23] Xueyu analyze numerical investigation on the heat and mass transfer in micro channel with discrete heat sources considering the Soret and Dufour effects [24]. Moghimi establish Heat transfer of MHD flow over a Wedge with Surface of Mutable temperature [25].

Hussain investigate Numerical simulation of MHD two-dimensional flow incorporated with joule heating and nonlinear thermal radiation [26].

The study involving Magneto-hydrodynamic flow through a collapsible tube with mass and heat transfer can be used to solve practical problems in field like medicine, engineering and so on. However, the soret and dufour effects on heat and mass transfer through a collapsible elastic tube with spectral based collocation technique have received little attention. This type of problem focused on expanding knowledge on different numerical techniques and is critical for fluid flows in capillary tubes such as blood flow in arteries or veins. This can result inefficient transport of nutrients, waste products, and other substances throughout the body. Therefore this paper focused to investigate the combined effects of Soret-Dufour effect together with Joule heating on unsteady newtonian MHD flow with mass and heat transfer through a collapsible tube by using spectral collocation method.

2. Mathematical Formulation

This research article consider two dimension MHD flow with mass and heat transfer that takes place along r and z-directions, then u_r and u_z are velocity components in r and z direction respectively with B_0 as magnetic field strength and g is acceleration due to gravity. The qeometry of collapsible elastic tube is cylindrical whereby the z axis lies along the center of the tube. The Figure 1 below shows a sketch diagram of the research problem.

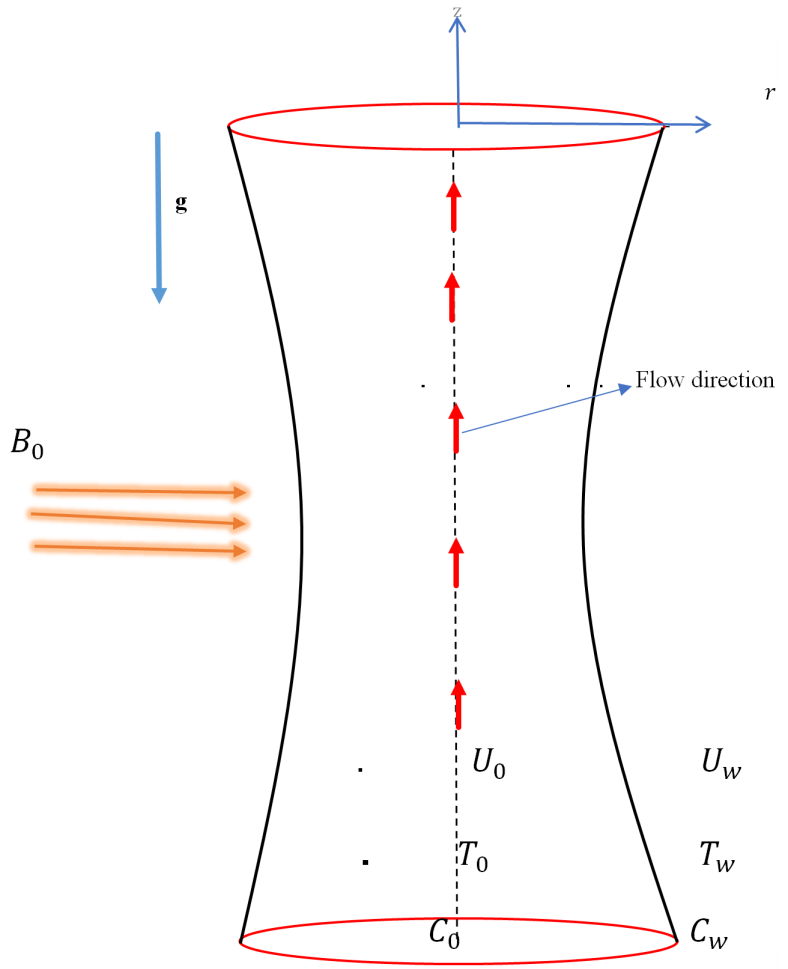

Figure 1. *Physical Model of the problem.*

The fluid flow is laminar and newtonian. The induced magnetic field, external electric field and Hall current are negligible. The difference in internal-external pressure is constant throughout the tube. The governing equations are continuity, momentum, energy and Concentration which are given respectively as:

Continuity equation:

$$\frac{\partial u_z}{\partial z} = 0 \tag{1}$$

Momentum equation:

$$\frac{\partial u_z}{\partial t} = \frac{\mu}{\rho}\left[\frac{\partial^2 u_z}{\partial r^2} + \frac{1}{r}\frac{\partial u_z}{\partial r}\right] - \frac{\sigma B_0^2 u_z}{\rho} + \beta^t g(T - T_w) + \beta^c g(C - C_w) \tag{2}$$

Energy equation:

$$\left(\frac{\partial T}{\partial t} + u_z\frac{\partial T}{\partial z}\right) = \frac{\kappa}{\rho C_p}\left(\frac{\partial^2 T}{\partial r^2} + \frac{1}{r}\frac{\partial T}{\partial r} + \frac{\partial^2 T}{\partial z^2}\right) + \frac{\mu}{\rho C_p}\left(\frac{\partial u_z}{\partial r}\right)^2 + \frac{\sigma u_z^2 B_0^2}{\rho C_p} + \frac{D_m K_t}{C_p C_s}\left(\frac{\partial^2 C}{\partial r^2} + \frac{1}{r}\frac{\partial C}{\partial r} + \frac{\partial^2 C}{\partial z^2}\right) \tag{3}$$

Concentration equation:

$$\frac{\partial C}{\partial t} = -u_z \frac{\partial C}{\partial z} + D_m \left[\frac{\partial^2 C}{\partial r^2} + \frac{1}{r}\frac{\partial C}{\partial r} + \frac{\partial^2 C}{\partial z^2} \right] - k_r (C - C_w) + \frac{D_m K_t}{T_m} \left(\frac{\partial^2 T}{\partial r^2} + \frac{1}{r}\frac{\partial T}{\partial r} + \frac{\partial^2 T}{\partial z^2} \right) \tag{4}$$

Boundary conditions considered are as follows.
At the centre line of the tube,

$$u_z = U_0, \qquad T = T_0 \qquad C = C_0 \qquad r = 0 \tag{5}$$

At the wall,

$$u_z = 0, \qquad T = T_W \qquad C = C_W \qquad r = a(t) \tag{6}$$

3. Similarity Transformation

The following non-dimensional transformation are used in the equation of continuity, equation of momentum, energy and concentration as used by ([20, 27–29])

$$u_z = -\frac{Q}{z} \cdot \frac{1}{\delta^{m+1}} f(\eta), \frac{\omega(\eta)}{\delta^{m+1}} = \frac{T - T_w}{T_0 - T_w}, \frac{\omega(\eta)_c}{\delta^{m+1}} = \frac{C - C_w}{C_0 - C_w}, \eta = \frac{r}{a_0} \tag{7}$$

Where $f(\eta)$ is the dimensionless velocity, $\omega(\eta)$ is the dimensionless temperature and $\omega(\eta)_c$ is the dimensionless concentration, T_0 is the temperature at the center of the tube,T_w is the temperature at the wall, C_0 is the Concentration at the center of the tube, C_w is the concentration at the wall, δ is the time dependent length scale and $\eta,\ m$ are arbitrary constant.
The following obtained,

$$f^{''}(\eta) + \frac{1}{\eta} f^{'}(\eta) + \frac{a_0^{m+1}(m+1)}{\delta^{m+1}} \lambda f(\eta) - \frac{\sigma B_0^2 a_0^2}{\mu} f(\eta) - \frac{a_0^2 z \delta^{m+1}}{vQ} \left[\beta^t g(T - T_w) + \beta^c g(C - C_w) \right] = 0 \tag{8}$$

$$-\frac{(m+1)a_0^{m-1}}{\delta^{m+1}} \lambda \omega(\eta) = \frac{\kappa}{\mu_0 C_p} \left(\frac{1}{a_0^2} \omega^{''}(\eta) + \frac{1}{a_0^2 \eta} \omega^{'}(\eta) \right) + \frac{1}{(T_0 - T_w) C_p} \left(\frac{Q^2}{a_0^2 z^2} \frac{1}{\delta^{(m+1)}} \right) \left(f^{'}(\eta) \right)^2 + \frac{\sigma B_0^2}{\mu_0 (T_0 - T_w) C_p} \frac{Q^2}{z^2 \delta^{(m+1)}} f^2(\eta) + \frac{D_m K_t}{\nu C_p C_s} \frac{(C_0 - C_w)}{(T_0 - T_w)} \left(\frac{1}{a_0^2} \omega^{''}(\eta)_c + \frac{1}{a_0^2 \eta} \omega^{'}(\eta)_c \right) \tag{9}$$

$$-\frac{\mu_0 a_0^{m-1}(m+1)}{\rho \delta^{2(m+1)}} \lambda \omega(\eta)_c = D_m \left(\frac{1}{a_0^2} \frac{\omega^{''}(\eta)_c}{\delta^{m+1}} + \frac{1}{a_0^2 \eta} \frac{\omega^{'}(\eta)_c}{\delta^{m+1}} \right) + \frac{D_m K_t}{T_m a_0^2} \frac{(T_0 - T_w)}{(C_0 - C_w)} \left(\frac{\omega^{''}(\eta)}{\delta^{m+1}} + \frac{1}{\eta} \frac{\omega^{'}(\eta)}{\delta^{m+1}} \right) - \frac{\Gamma \mu_0}{\rho a_0^2} \frac{\omega(\eta)_c}{\delta^{m+1}} \tag{10}$$

We introduce Non-dimensional parameters which arise from the problem as listed below:

$$Re = \frac{Ua}{\nu}, Pr = \frac{C_p \mu}{\kappa}, Ec = \frac{U^2}{C_p \triangle T}, Ha = a_0 B_0 \sqrt{\frac{\sigma}{\mu}}, Gr = \frac{g \beta^t (T_w - T_0) a_0^3}{\nu^2}, +$$

$$Gc = \frac{g \beta^c (C_w - C_0) a_0^3}{\nu^2}, Sc = \frac{\mu}{\rho D_m}, Sr = \frac{D_m K_{t(T-T_w)}}{T_m (C - C_w) \nu}, Du = \frac{D_m K_{t(C-C_w)}}{C_p C_s (T - T_w) \nu}, \Gamma = k_r \frac{\rho a^2}{\mu}, \lambda = \frac{\rho \delta^m}{\mu a^{m-1}} \frac{d\delta}{dt}. \tag{11}$$

Where Re is Reynolds number, Pr is Prandtl number, Ec is Eckert number, Ha is Hartmann number, Gr is Thermal Grashof number, Gc is Concentration Grashof number, Sc is Schmidt number, Sr is Soret number, λ is Unsteadiness parameter and Du is Dufour parameter. By substituting equation (11), in equations (8)-(10) the following set of ODEs obtained

$$f^{''}(\eta) + \frac{1}{\eta} f^{'}(\eta) + \frac{a_0^{m+1}(m+1)}{\delta^{m+1}} \lambda f(\eta) - Ha^2 f(\eta) - \frac{z}{a_0^2 Re} \left[\omega(\eta) Gr + \omega(\eta)_c Gc \right] = 0 \tag{12}$$

$$\frac{1}{Pr} \omega^{''}(\eta) + \frac{1}{Pr \eta} \omega^{'}(\eta) + \frac{(m+1)a_0^{m+1}}{\delta^{m+1}} \lambda \omega(\eta) + Du \omega^{''}(\eta)_c + Du \frac{1}{\eta} \omega^{'}(\eta)_c + \frac{Ec}{z^2 \delta^{m+1}} \left(f^{'}(\eta) \right)^2 + \frac{Ha^2 Ec}{z^2 \delta^{m+1}} f^2(\eta) = 0 \tag{13}$$

$$\frac{1}{Sc}\frac{\omega^{''}(\eta)_c}{\delta^{m+1}}+\frac{1}{Sc}\frac{\omega^{'}(\eta)_c}{\eta\delta^{m+1}}+\left(\frac{a_0^{m+1}(m+1)}{\delta^{2(m+1)}}\lambda-\Gamma\frac{1}{\delta^{m+1}}\right)\omega(\eta)_c+Sr\frac{\omega^{''}(\eta)}{\delta^{m+1}}+Sr\frac{1}{\eta}\frac{\omega^{'}(\eta)}{\delta^{m+1}}=0 \tag{14}$$

The transformed Boundary conditions are as follows,
At the centre line:

$$f(0)=-z\delta^{m+1} \qquad \omega(0)=\delta^{m+1} \qquad \omega(0)_c=\delta^{m+1} \qquad if\ \ \eta=0 \tag{15}$$

At the wall:

$$f(0)=-z\delta^{m+1} \qquad \omega(0)=\delta^{m+1} \qquad \omega(0)_c=\delta^{m+1} \qquad if\ \ \eta=0 \tag{16}$$

The skin friction, the Nusselt number and Sherwood number are defined by [9]

$$C_f=\frac{\tau_w}{\rho U_0^2} \qquad Nu=\frac{a_0 q_h}{k(T_0-T_w)} \qquad Sh=\frac{a_0 q_m}{D_m(C_0-C_w)} \tag{17}$$

Where τ_w is the skin shear stress on the surface, q_h is the heat flux, q_m is the mass flux defined by (18) below

$$\tau_w=\mu\frac{\partial u}{\partial r}\bigg|_{r=0}, \qquad q_h=-\kappa\frac{\partial T}{\partial r}\bigg|_{r=0}, \qquad q_m=-D_m\frac{\partial C}{\partial r}\bigg|_{r=0} \tag{18}$$

By substituting equation (7) in (17) following obtained

$$C_f=Re^{-1}f^{'}(\eta), \qquad Nu=\frac{-\omega^{'}(\eta)}{\delta^{m+1}} \qquad Sh=\frac{-\omega^{'}(\eta)_c}{\delta^{m+1}} \tag{19}$$

4. Numerical Solution Procedure

Collocation method is the numerical technique used for solving PDEs by discretizing the PDEs using a set of collocation points. Method based on the idea of approximating the solution of PDE by a polynomial function that satisfies PDE at a finite number of selected points called collocation points. The collocation method can be applied using different types of basis functions such as polynomial, trigonometric etc. The choice of basis function depend on the nature ofPDEs and geometry of the problem. This method makes use of solvers with low computation memory that making it easy to implement in MATLAB code using BVP4C inbuilt function. This method is the best to solve BVP than any other numerical technique since is easy to implement and it is also referred as Pseudo Collocation. The collocation method can be represented mathematically as:
Consider PDE of the form.

$$\mathbf{L}(u(x))=\mathbf{F}(x) \qquad x\in[a,b] \tag{20}$$

where $\mathbf{L}$ is linear differential operator, $y(x)$ is unknown function to be solved, $\mathbf{F}(x)$ is a given function. The Collocation method seek an approximation of the solution $U(x)$ using linear combination of the basis functions $\phi_i(x)$ is obtained by

$$u(x)\approx U(x)=\sum_{j=1}^{N}c_i\phi_j(x) \tag{21}$$

such that

$$\sum_{j=1}^{N}c_j\phi_j(a)=\alpha, \qquad \sum_{j=1}^{N}c_j\phi_j(b)=\beta \tag{22}$$

Where $c_1,...,c_N$ are unknown coefficients
To obtain $N-2$ equations,$N-2$ collocation points are chosen in such a way that they represent the behavior of the solution over the whole interval
Letting $x_1=a$ and $x_N=b$ then

$$\sum_{j=1}^{N}c_j\phi_j(x_1)=\alpha, \qquad \sum_{j=2}^{N}c_j\phi_j(x_j)=r(x_j), \qquad \sum_{j=1}^{N}c_j\phi_j(x_N)=\beta, j=2,3,...,N-1 \tag{23}$$

The linear system is represented in matrix form as:

$$\begin{bmatrix} \phi_1(x_1) & \phi_2(x_1) & . & . & \phi_N(x_1) \\ \phi_1(x_2) & \phi_2(x_2) & . & . & \phi_N(x_2) \\ \phi_1(x_3) & \phi_2(x_3) & . & . & \phi_N(x_3) \\ . & & & . & \\ . & & & . & \\ . & & & . & \\ \phi_1(x_{N-1}) & \phi_2(x_{N-1}) & . & . & \phi_N(x_{N-1}) \\ \phi_1(x_N) & \phi_2(x_N) & . & . & \phi_N(x_N) \end{bmatrix} \begin{bmatrix} c_1 \\ c_2 \\ c_3 \\ . \\ . \\ . \\ c_{N-1} \\ c_N \end{bmatrix} = \begin{bmatrix} \alpha \\ r(x_2) \\ r(x_3) \\ . \\ . \\ . \\ r(x_{N-1}) \\ \beta \end{bmatrix}$$

If the above matrix is non-singular then the approximate solution from the space**U** is unique and represented as,

$$u(x) \approx U(x) = \sum_{j=1}^{N} c_j \phi_j(x) \qquad x \in [a, b] \tag{24}$$

In this study we are going to use Lagrange basis and Chebyshev-Gauss-Lobatto collocation points. This is because the Differentiation matrices due to lagrange basis and Chebyshev-Gauss-Lobatto collocation points are explicitly defined by Trefethen. That is there exist explicit formula for the entries of Differentiation matrix **D** where lagrange basis are used [30].

The solution of the differential equations are assummed to be Lagrange interpolation polynomial of the form

$$\begin{aligned} f(\eta) &= \sum_{j=0}^{N} L_j(\eta) f_j \\ \omega(\eta) &= \sum_{j=0}^{N} L_j(\eta) \omega_j \\ \omega(\eta)_c &= \sum_{j=0}^{N} L_j(\eta) (\omega_j)_c \end{aligned} \tag{25}$$

Where $f_j = f(\eta_j)$, $\omega_j = \omega(\eta_j)$, $(\omega_j)_c = \omega(\eta_j)_c$ and $N+1$ are number of grid points.
The grid points are Chebyshev-Gauss-Lobatto nodes defined on the interval $[-1, 1]$ by

$$z_i = \cos\left(\frac{i\pi}{N}\right) \qquad for \;\; i = 0, 1, 2, ..., N \tag{26}$$

Usually linear transformation is used to map interval [-1,1] to computational domain $\eta = [0, 1]$ then we get

$$\eta_i = \frac{1}{2}(z_i + 1)$$

The first derivative of $f(\eta)$ at the grid points is approximated as follows

$$\begin{aligned} f^{'}(\eta) &= \sum_{j=0}^{N} L_j^{'}(\eta) f_j \\ f^{'}(\eta_i) &= \sum_{j=0}^{N} L_j^{'}(\eta_i) f_j \\ &= \sum_{j=0}^{N} D_{ij}(\eta) f_j \qquad i = 0, 1, 2, ..., N \end{aligned} \tag{27}$$

Where $D_{ij} = L_j^{'}(\eta_i)$ and D is a Chebyshev differentiation matrix as defined by [30]
then

$$\mathbf{F}^{'} = D\mathbf{F} \tag{28}$$

where $\mathbf{F} = [f(\eta_0), f(\eta_1), ..., f(\eta_N)]^{\mathbf{T}}$
Higher order derivatives are approximated by $F^{''} = D^2 F$. Now for the the transformed equations.

For Velocity:

$$\left[D^2 + \frac{1}{\eta} D + \left(\frac{(m+1)a_0^{m+1}\lambda}{\delta^{m+1}} - Ha^2\right) I\right] F = R_1 \tag{29}$$

where

$$R_1 = \frac{z}{a_0^2 Re}[\omega(\eta) Gr + \omega(\eta)_c Gc]$$

then

$$A_1 F = R_1$$

For Temperature:

$$\left[\frac{1}{Pr} D^2 + \frac{1}{Pr\eta} D + \left(\frac{(m+1)a_0^{m+1}\lambda}{\delta^{m+1}}\right) I\right] W = R_2 \tag{30}$$

where

$$R_2 = -\left[Du\omega^{''}(\eta)_c + \frac{Du}{\eta}\omega^{'}(\eta)_c + \frac{Ec}{z^2\delta^{m+1}}(f^{'}(\eta)^2) + \frac{Ha^2 Ec}{z^2\delta^{m+1}} f^2(\eta)\right].] \tag{31}$$

then

$$A_2 W = R_2$$

For Concentration:

$$\left[\frac{1}{Sc\delta^{m+1}}D^2 + \frac{1}{Sc\eta\delta^{m+1}}D + \left(\frac{(m+1)a_0^{m+1}}{\delta^{2(m+1)}} - \frac{\Gamma}{\delta^{m+1}}\right)I\right]W_c = R_3 \tag{32}$$

Where

$$R_3 = -\frac{Sr}{\delta^{m+1}}\omega^{''}(\eta) + \frac{Sr}{\eta\delta^{m+1}}\omega^{'}(\eta)$$

then

$$A_3 W_c = R_3$$

With boundary conditions

$$\begin{aligned} &f(\eta) = 0 \qquad \omega(1) = 0 \qquad \omega(1)_c = 0 \quad if \;\; \eta = 1 \\ &f(0) = -z\delta^{m+1} \qquad \omega(0) = \delta^{m+1} \qquad \omega(0)_c = \delta^{m+1} \quad if \;\; \eta = 0 \end{aligned} \tag{33}$$

5. Results and Discussion

The numerical solutions of the model's velocity, temperature, and concentration profiles while varying various dimensionless parameters. The effect of each parameter has been discussed at each stage.

5.1. Velocity Profiles

5.1.1. Effects of Reynolds Number (Re) on Velocity

From Figure 2, it observed that velocity of the fluid in the flow region increase with increase in the value of Reynolds number. This is due to the reason that increase in Reynolds number leads to decrease of viscosity of the fluid decreases. A decrease in viscosity of the of the fluid leads to reduce in viscous force in the flow and therefore inertia forces dominates. Since we know that viscous forces tend to oppose the motion of the flowing fluid. Also the velocity boundary layer does not extend more in the free stream region hence increase in fluid velocity. Conversely when viscous forces predominate, Reynolds number reduces leads to decrease in velocity profiles.

5.1.2. Effects of Hartman Number (Ha) on Velocity

In Figure 3 it shows that decrease in Hartman number leads to increase in velocity profiles. An increase in Hartman number leads to decrease velocity of the fluid, this is due to the fact that the presence of uniform magnetic field applied perpendicular to the flow direction of electrically conducting fluid leads to induction of Lorentz force. When Hartman increase cause the increase in the Lorentz force which is against the fluid flow direction causes the fluid's flow to slow down.

5.1.3. Effects of Unsteadiness Parameter (λ) on Velocity

Considering velocity profile Figure 4 it has been observed that increase in unsteadiness parameter increases velocity profiles. An increase in unsteadiness parameter leads to reduce kinematic viscosity. Hence increase in fluid velocity. Unsteadiness parameter brings about the issue of unsteady state of the flow and time-dependent scale.

5.1.4. Effects of thermal Grashof Number (Gr) on Velocity

From Figure 5, it depicted that velocity profiles increases as Grashof number for heat transfer increases. From definition of Grashof number for heat transfer is a ratio of the thermal buoyancy force to the viscous force. So when Grashof number increase lead to reduction in viscosity then viscous force hence increase in thermal bouyancy force which lead to an increase in velocity.

5.1.5. Effects of Concentration Grashof Number (Gc) on Velocity Profiles

From Figure 6, it has illustrated that velocity profiles of the flow rise up with an increase in the Grashof number for mass transfer (Gc). Since Grashof number for mass transfer is represented by ratio of the solutal buoyancy force to the viscous force. Increasing Grashof number leads to decrease in the viscosity of the fluid which results to decrease in the viscous force which results to an increase in the species buoyancy force and hence increase the velocity profiles.

5.2. Temperature Profiles

5.2.1. Effects of Dufour Number (Du) on Temperature

In Figure 7, it has been illustrated that rise in dufour parameter leads to rise in temperature distributions. Dufour parameter is the thermal energy transfer simply (energy flux) induced by mass concentration gradient, increase in dufour

number generate heat energy flux which lead to increase in thickness of thermal boundary layer this lead slow travel of heat energy, resulting the fluid temperature to rise. This is due to the fact that dufour number is proportional to the temperature differences between wall and fluid.

5.2.2. Effects of Reynolds (Re) Number on Temperature

Figure 8, it found that rise in Reynolds number parameter results into raises in temperature profiles. An increase in Reynolds number leads to the enhanced rates of shearing and consequently the viscous dissipation effects. From literature temperature raises tend to reduce viscous force, thus when viscosity reduce inertia force become predominant since Reynolds parameter is the ratio of the inertial forces to viscous forces. Hence there is direct relation between temperature and Reynolds parameter.

5.2.3. Effects of Eckert Number (Ec) on Temperature

Figure 9 below it shows that addition in Eckert number leads to raise in temperature profiles. This is because joule heating and viscous dissipation increase as a result of increasing fluid velocity. The velocity is highest at the centre of tube and so viscous dissipation effects. In this case when there is high conversion of kinetic energy into internal energy fluid velocity being high due to fluid particles are in a constant collision and particles vibration becomes high. A rise in this Eckert number translates into rise kinetic energy of the fluid particles. This lead to rise the random movement of the fluid particles results to collision and generates thermal energy thereby making the fluids temperature to rise.

5.2.4. Effects of Hartman Number (Ha) on Temperature

Figure 10 depict that the temperature distribution raises with amplifying in Hartman number. This increase in Hartman parameter means that magnetic force dominates and viscous forces reduces. The increased magnetic force leads to thermal boundary layer to increase since the thermal boundary layer formed extends into the free stream region which in turn leads to an increased fluid temperature. From literature we know that viscosity and temperature are inversely proportional and when viscosity reduces, this leads to increase of temperature of the fluid flow in the flow region. Also an increase in Hartman number leads to an increase in joule heating from induced electric current. The temperature drops towards the wall of the tube due to the low velocities near the wall which results in the low joule heating.

5.2.5. Effects of Soret Number (Sr) on Temperature

From Figure 11, it is obseved that temperature decreases when soret number increase. This is due to soret number signifies the contribution of the temperature gradient to the mass flux in the fluid flow. Temperature decrease with increase soret number due to it reduce profiles of concentration which leads to increase in mass transfer in the flow.

5.2.6. Effects of Schmidit (Sc) Number on Temperature

From Figure 12, It found that an increase in Schmidit number cause a considerable reduction in temperature profiles. From definition Schimdit number is the ratio of kinematic viscosity to the mass diffusitivity. An increase in Schimdit number decrease the mass diffusitivity which results to increase in viscous force of the fluid and increase in viscocity will leads to raise in temperature profiles of the fluid.

5.3. Concentration Profiles

5.3.1. Effects of Dufour Number (Du) on Concentration

Figure 13 below it is noted that when there is decrease in dufour number results into increase in concentration profiles. This is because increase in dufour number, temperature gradient effect between the wall and fluid decreases leads to more heat in fluid. Hence Concentration profiles decrease

5.3.2. Effects of Chemical Reaction Parameter (Γ) on Concentration

In Figure 14 it was illustrated that addition in chemical reaction parameter leads to reduce concentration profiles. This is due to increase in chemical reaction reduces amount of species in fluid hence the movement of species decrease. When chemical reaction occur species are consumed during reaction process. Also it is caused by the negative chemical reaction which reduces or decreases the concentration boundary layer thickness and increases the mass transfer.

5.3.3. Effects of Eckert Number (Ec) on Concentration

Figure 15 below, it found that decrease in Eckert number increase concentration profile. An increase in Eckert parameter can lead to enhanced heat transfer, which affects the reaction rates. Higher temperatures resulting from increased heat transfer can accelerate chemical reactions, leading to changes in decreasing concentration profiles. Therefore concentration profiles increase as the results of reducing in Eckert number.

5.3.4. Effects of Soret Number (Sr) on Concentration

Figure 16, It has been noted that increase in Soret number reduces concentration profiles. This dimensionless number explain the mass species are separeted in the mixture which is driven by temperature gradient of the flow.

5.3.5. Effects of Schmidt Number (Sc) on Concentration

From Figure 17, it is observed that concentration profiles reduced as the Schmidit number increases. This is due to increase in Schmidit number reduces the mass diffusivity as they are in inverse relation which results to decrease in the concentration profiles of the fluid.

5.3.6. Effects of Concentration Grashof Number (Gc) on Concentration

From Figure 18 It has illustrated that increase in Grashof number for mass transfer leads to decrease concentration profiles. This is due to increase in Grashof number increases in concentration gradient which tend to enhance mass buoyancy effect. The mass buoyanc effect is more at the centre of tube and less toward the wall then reduces the concentration profiles.

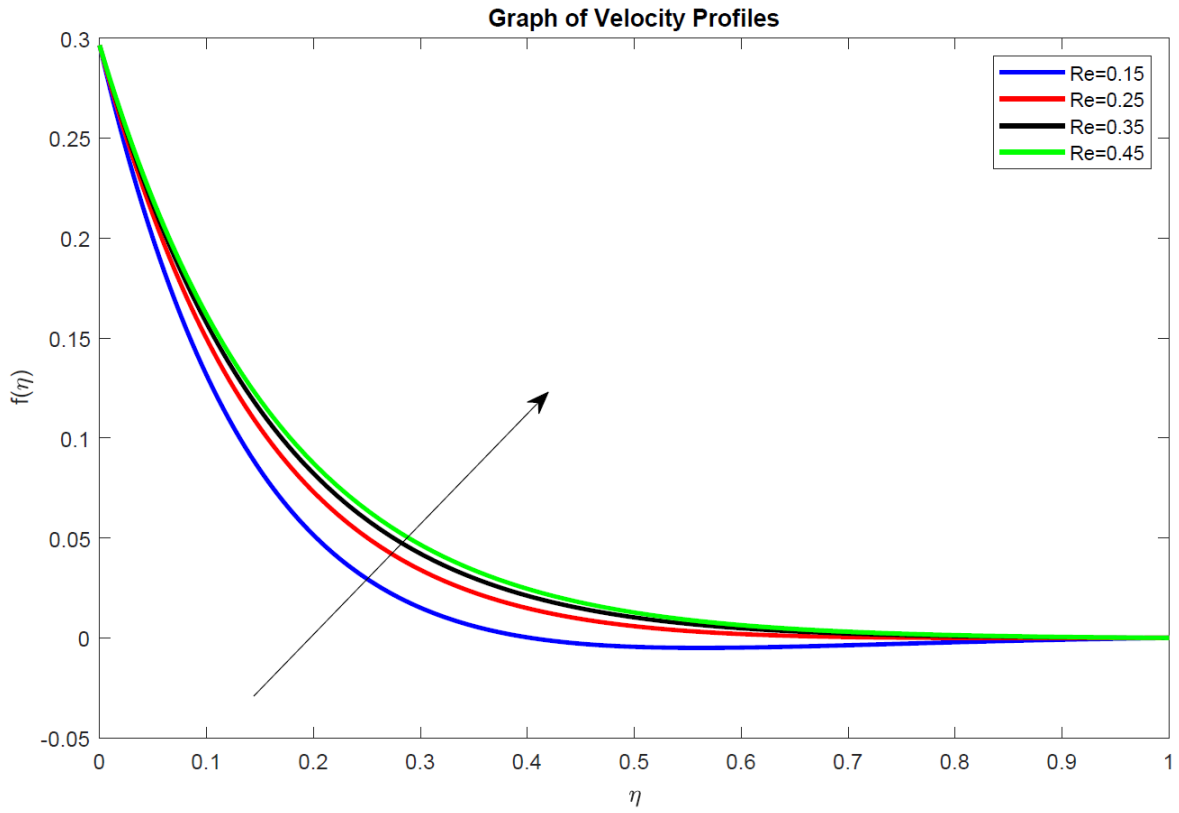

Figure 2. *Velocity profiles for different values of Re.*

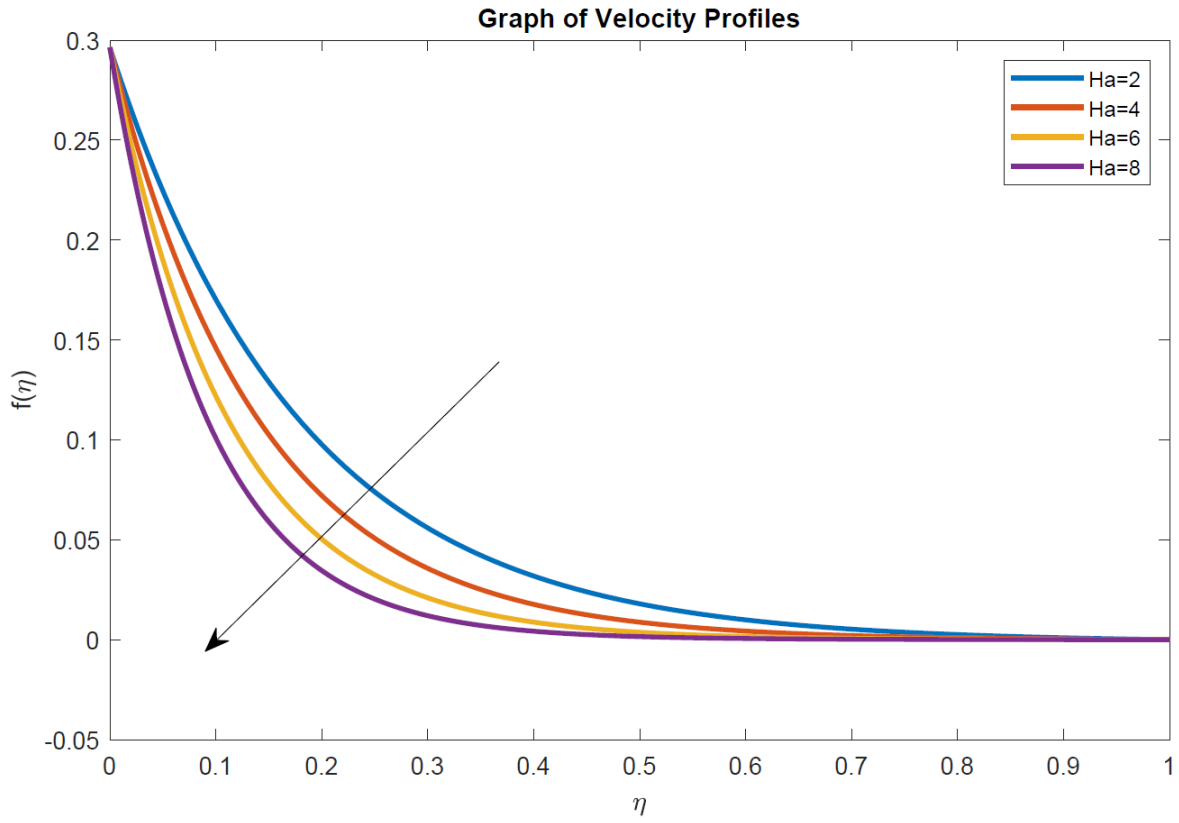

Figure 3. *Velocity profiles for different values of Ha.*

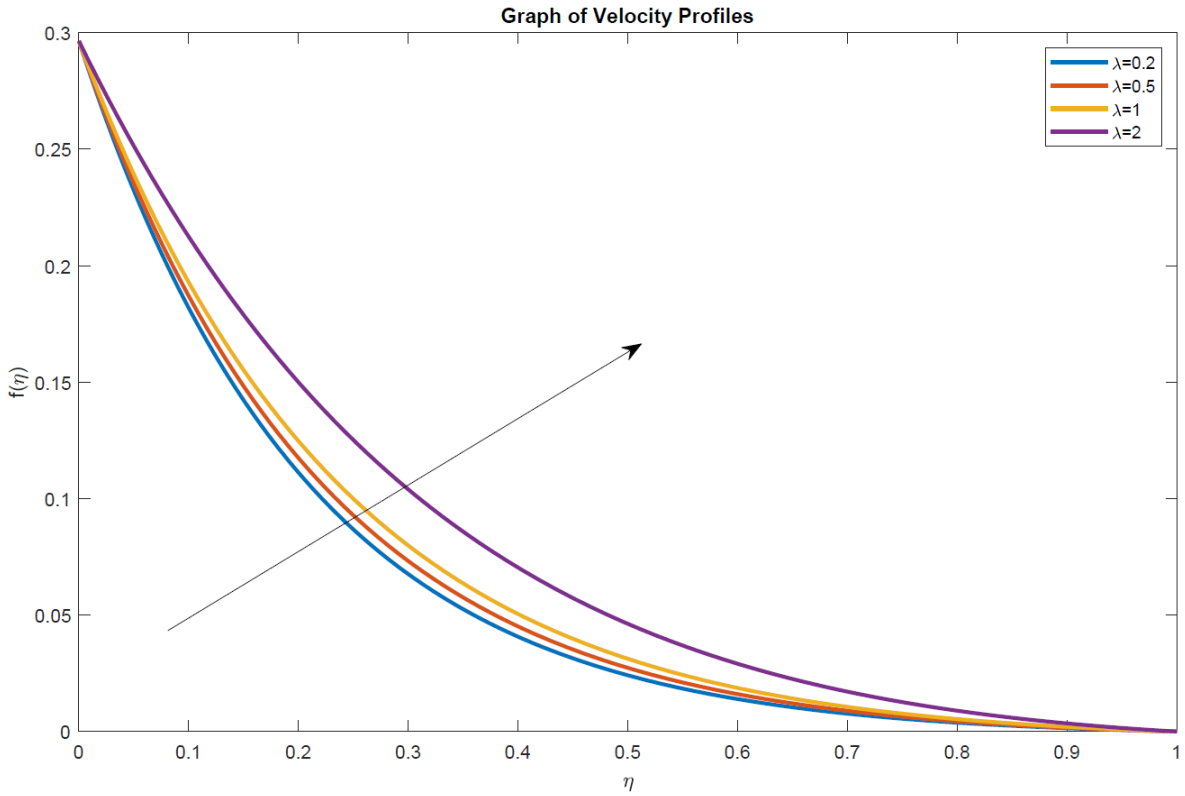

Figure 4. *Velocity profiles for different values of λ.*

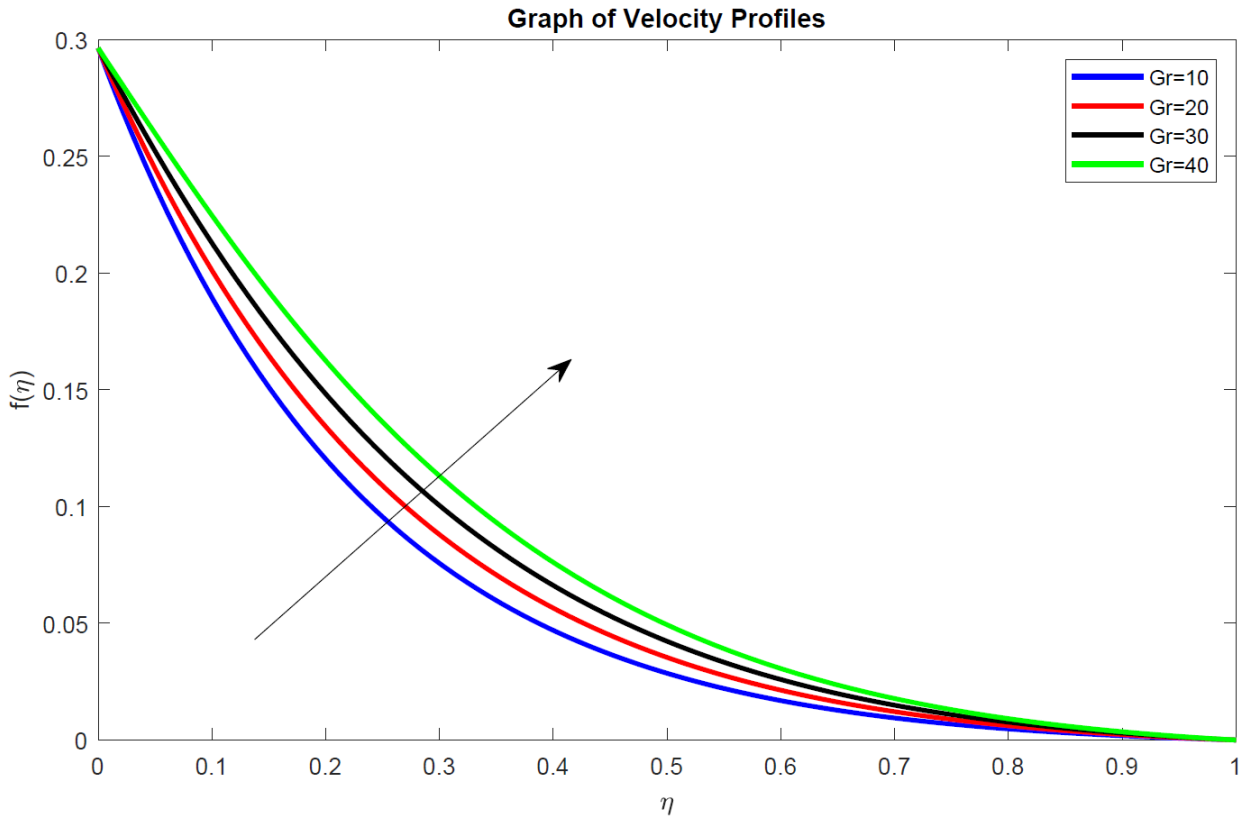

Figure 5. *Velocity profiles for different values of Gr.*

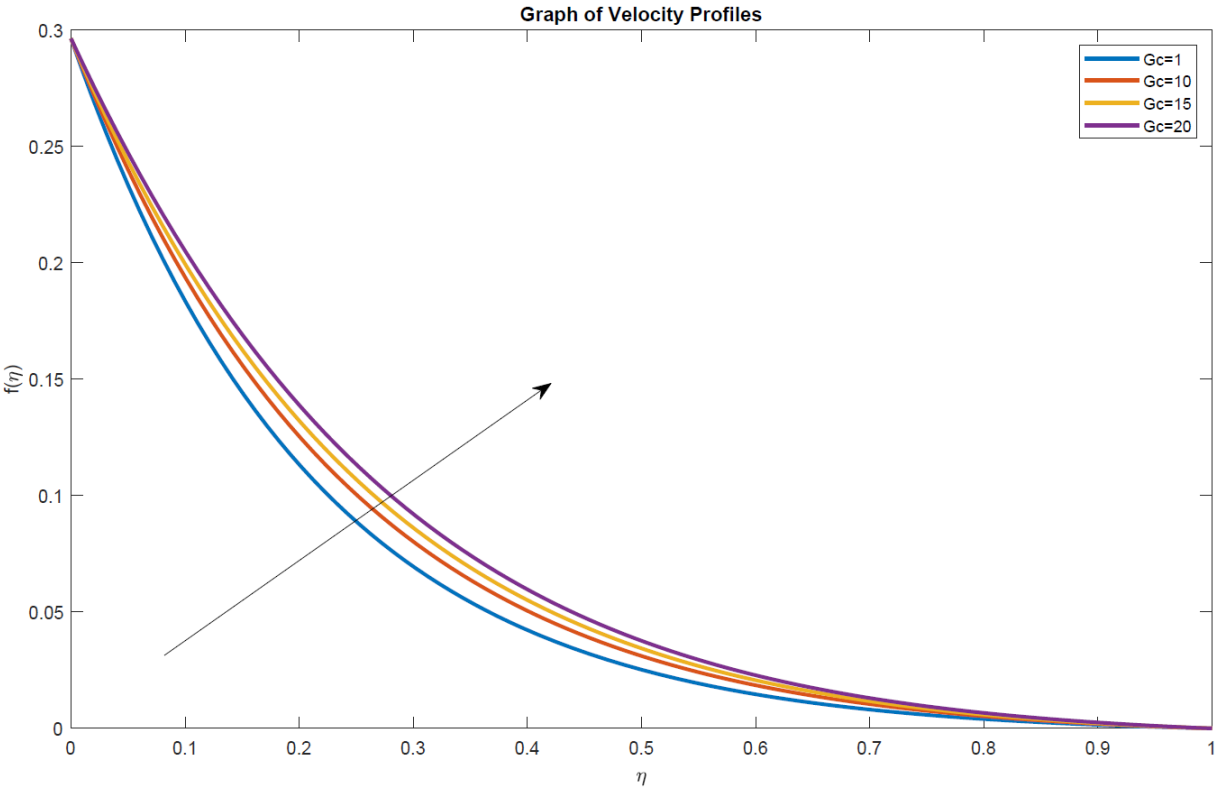

Figure 6. *Velocity profiles for different values of Gc.*

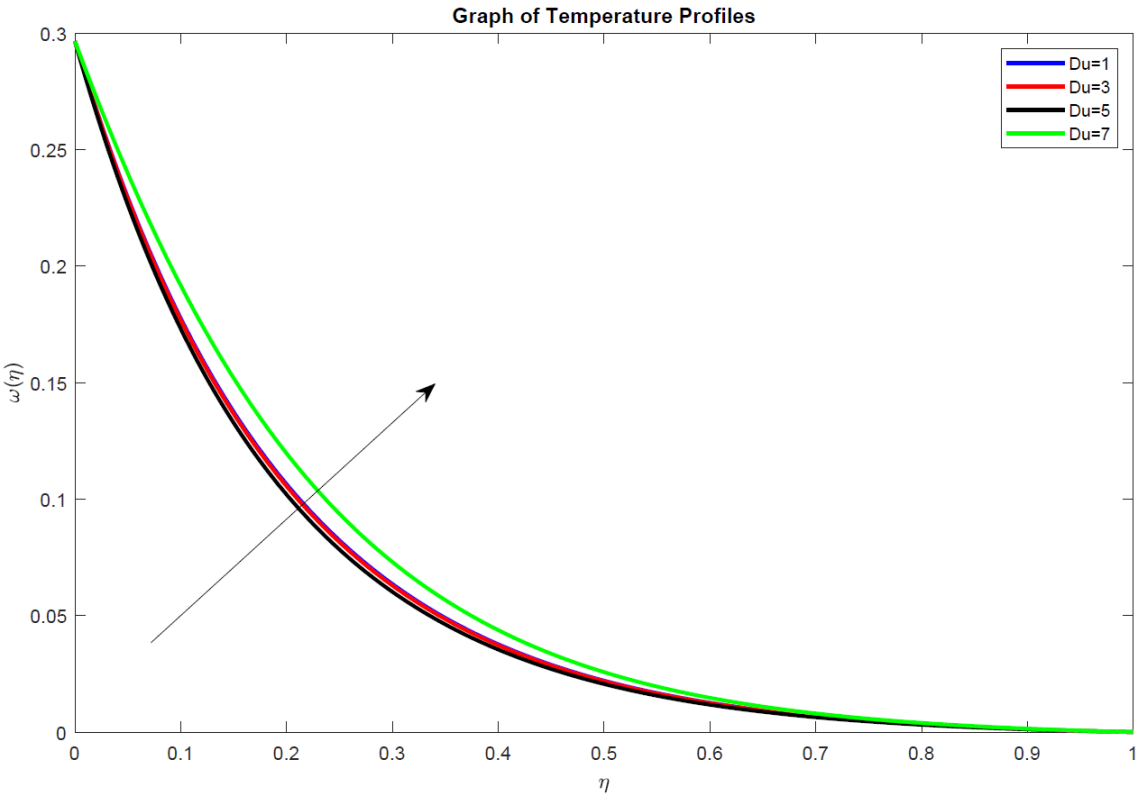

Figure 7. *Temperature profiles for different values of Du.*

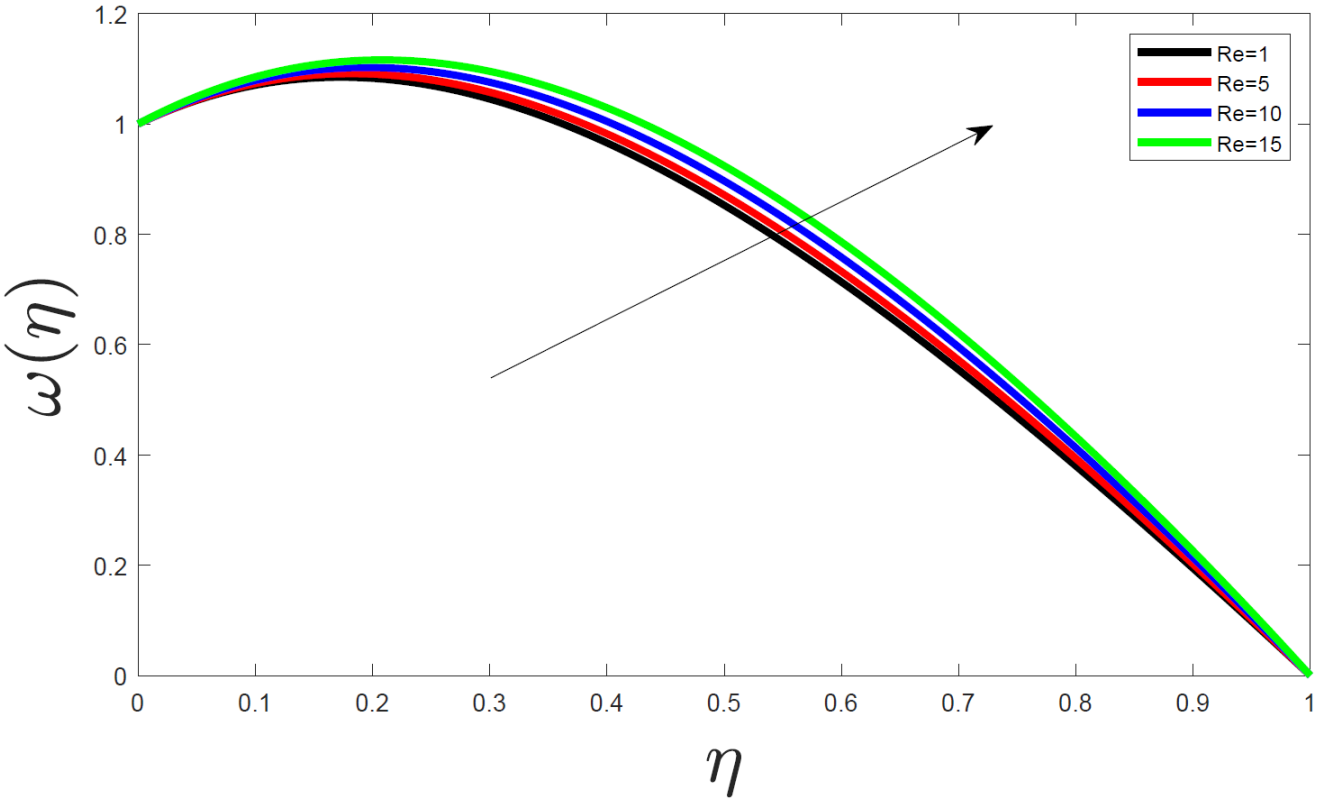

Figure 8. *Temperature profiles for different values of Re.*

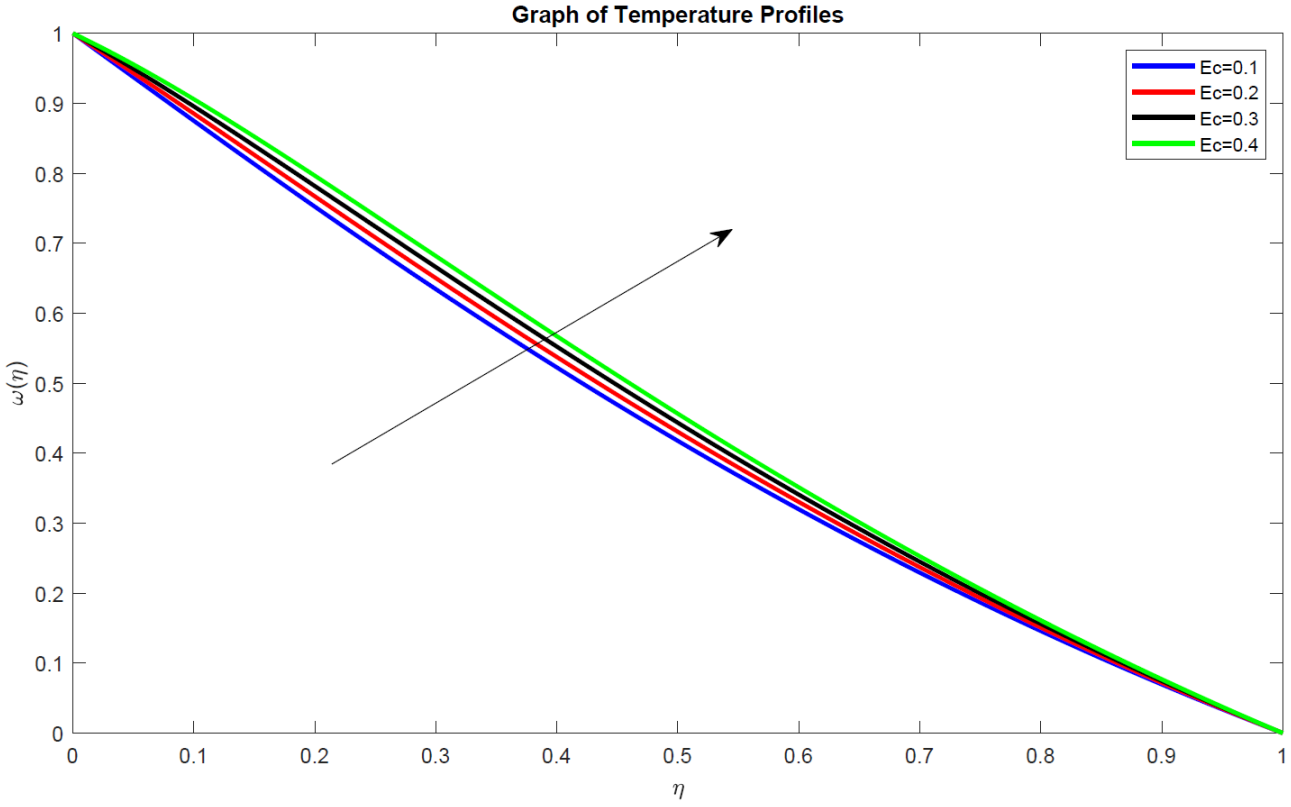

Figure 9. *Temperature profiles for different values of Ec.*

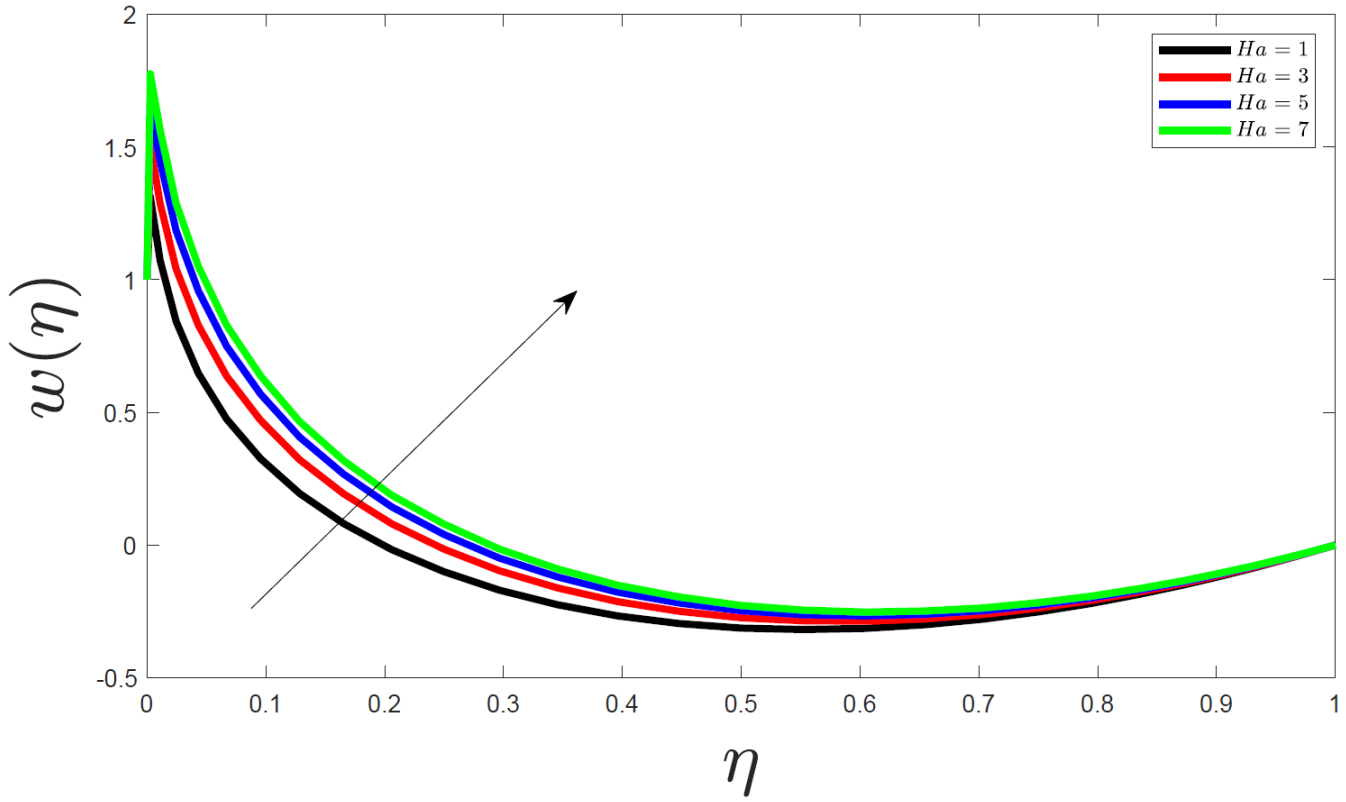

Figure 10. *Temperature profiles for different values of Ha.*

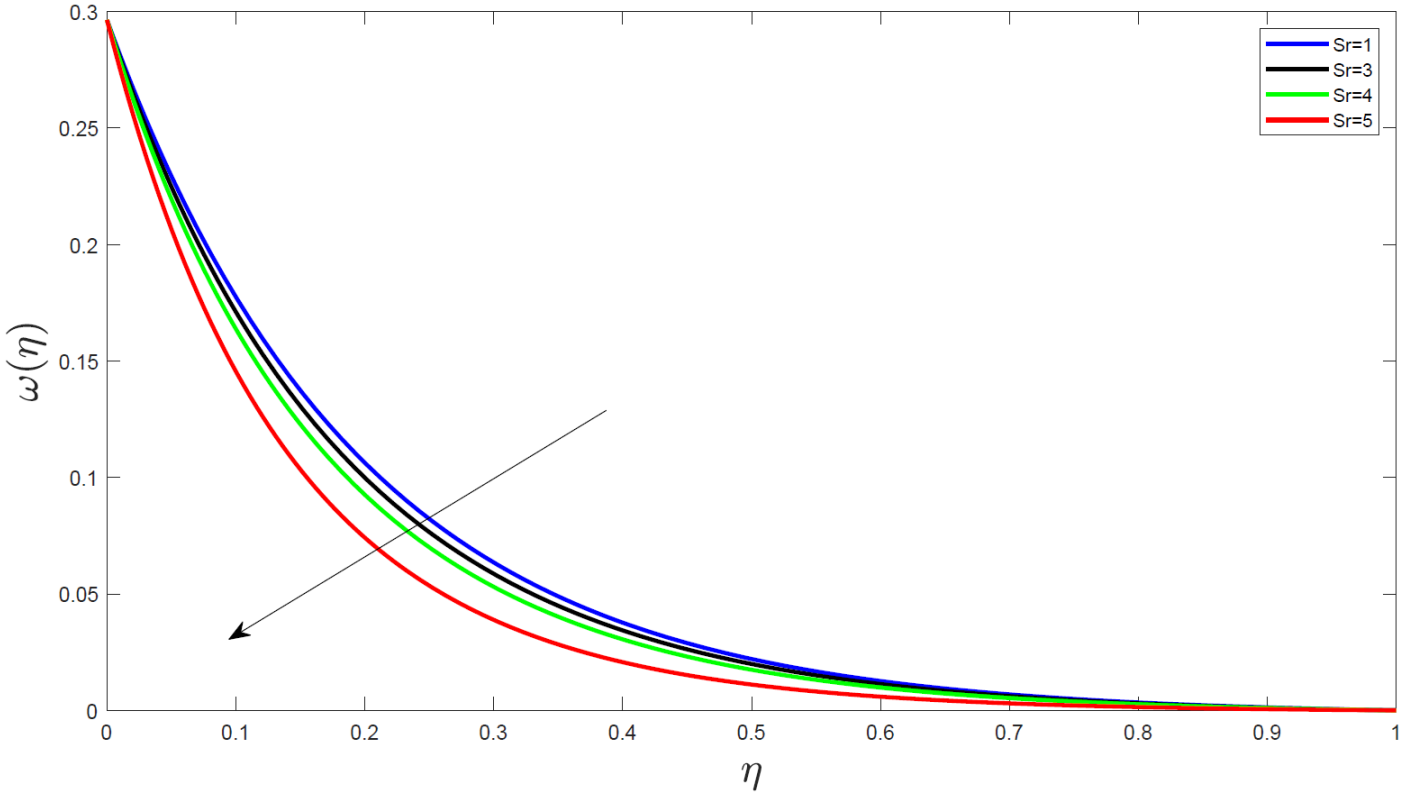

Figure 11. *Temperature profiles for different values of Sr.*

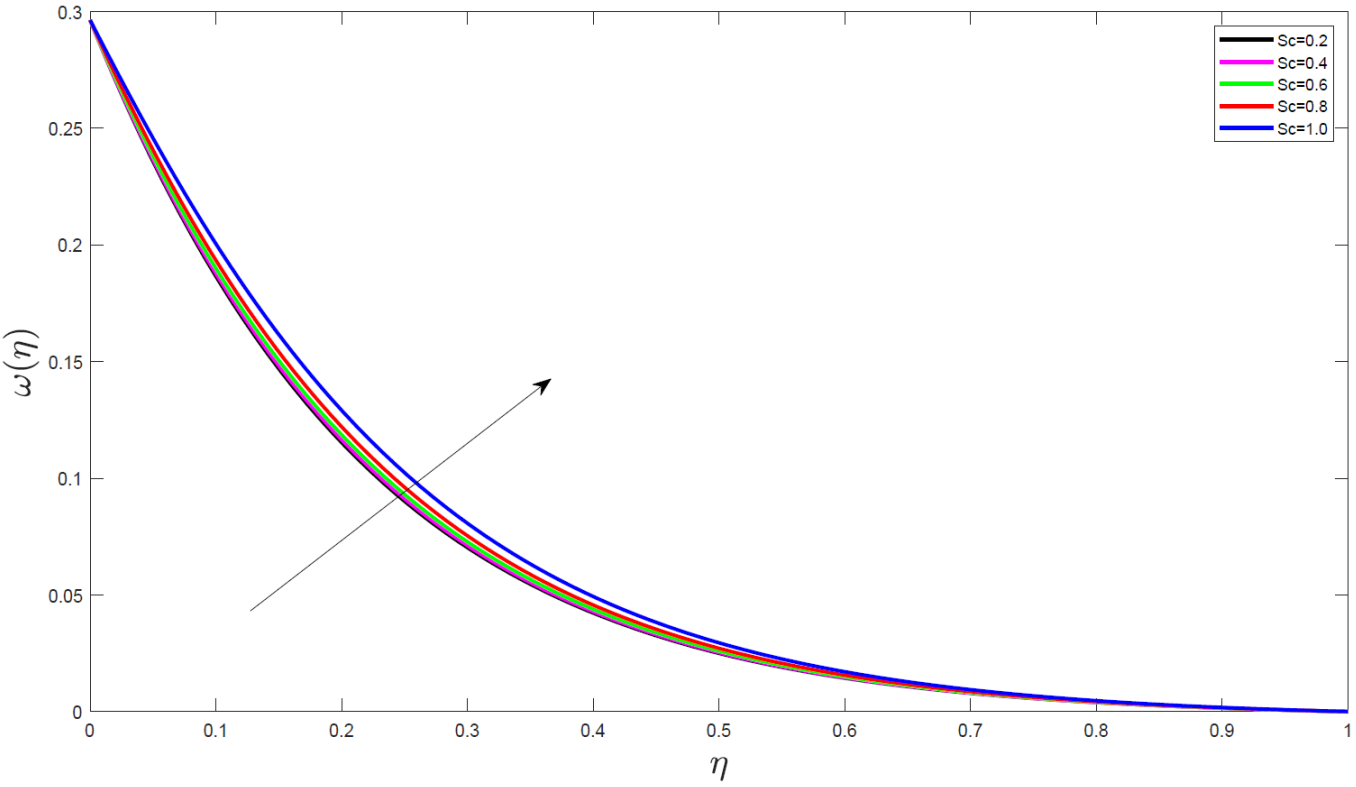

Figure 12. *Temperature profiles for different values of Sc.*

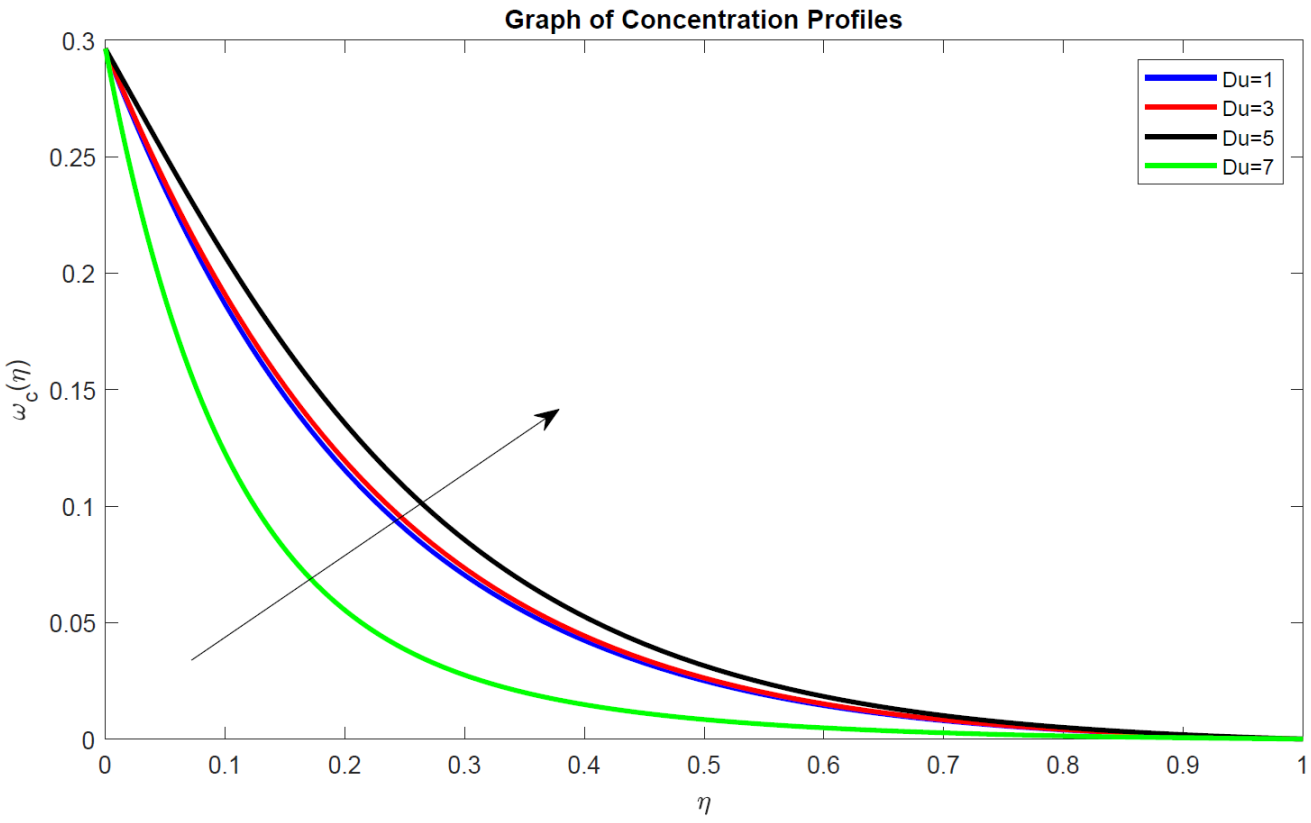

Figure 13. *Concentration profiles for different values of Du.*

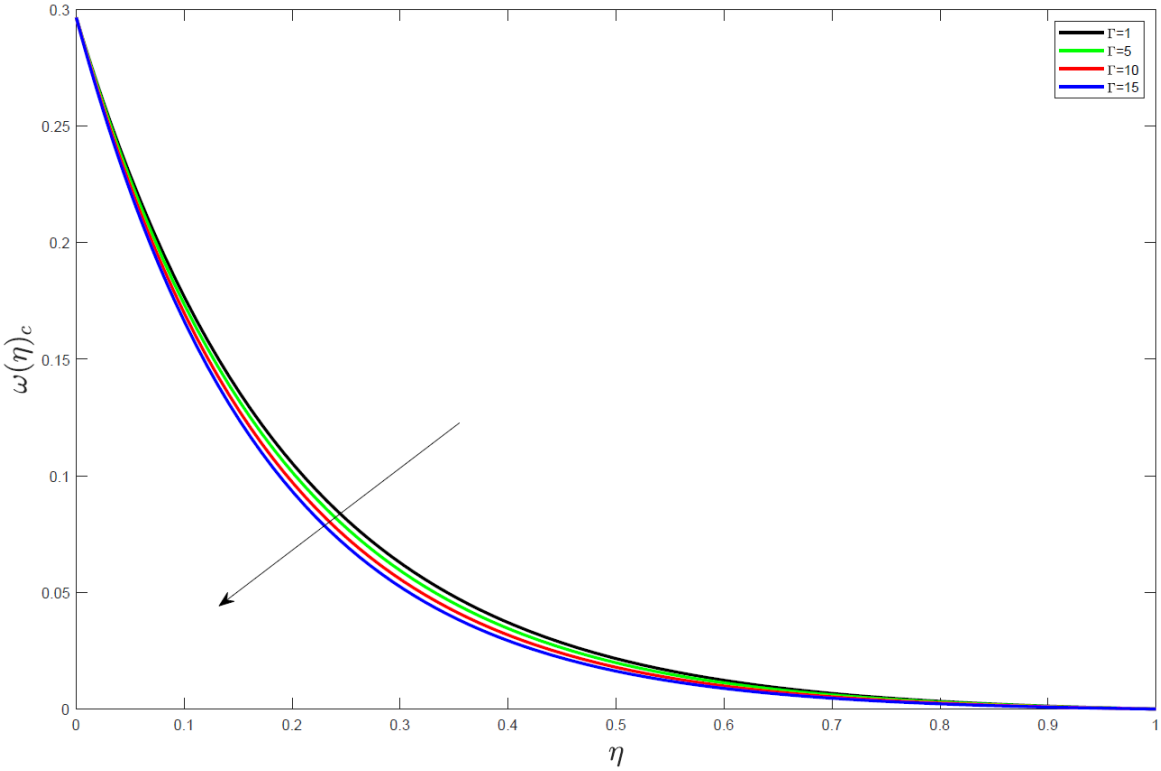

Figure 14. *Concentration profiles for different values of* Γ.

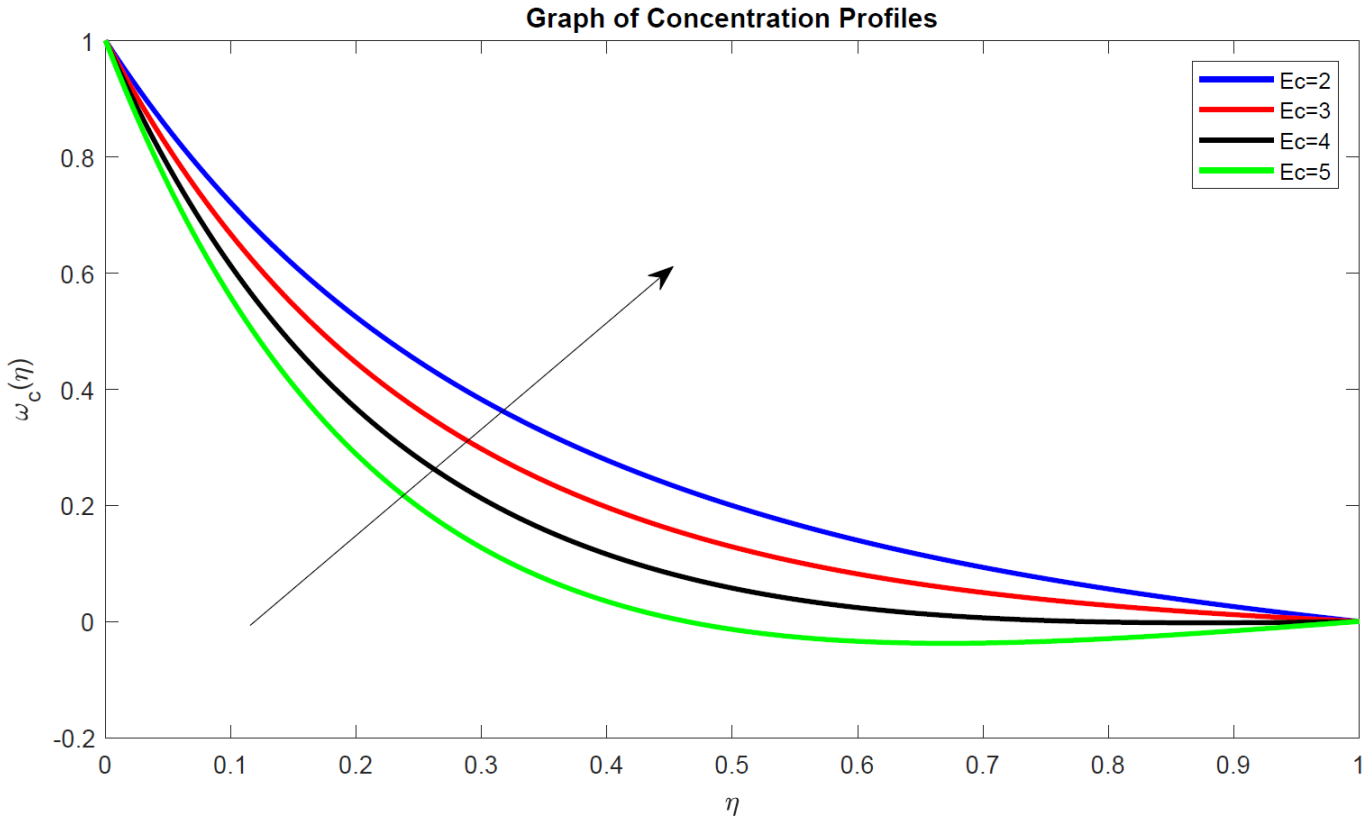

Figure 15. *Concentration profiles for different values of* Ec.

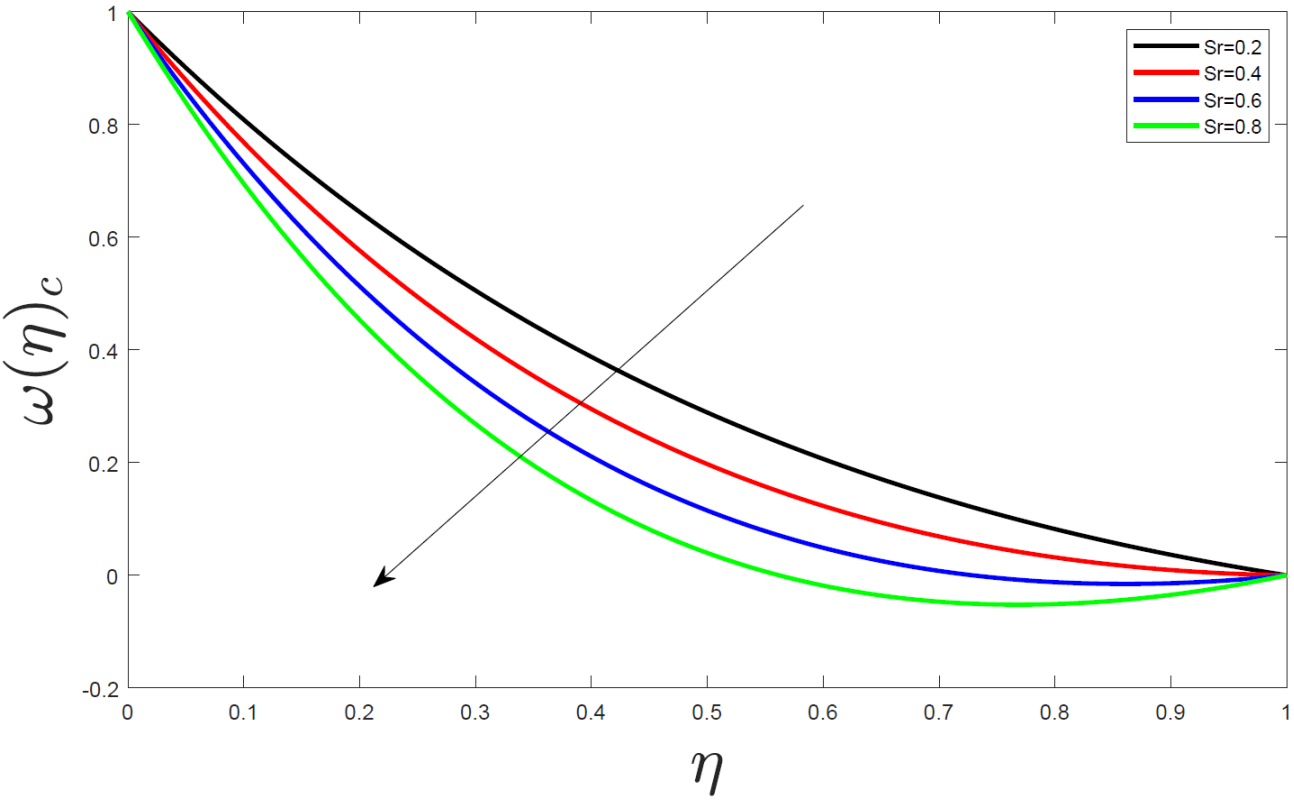

Figure 16. *Concentration profiles for different values of Sr.*

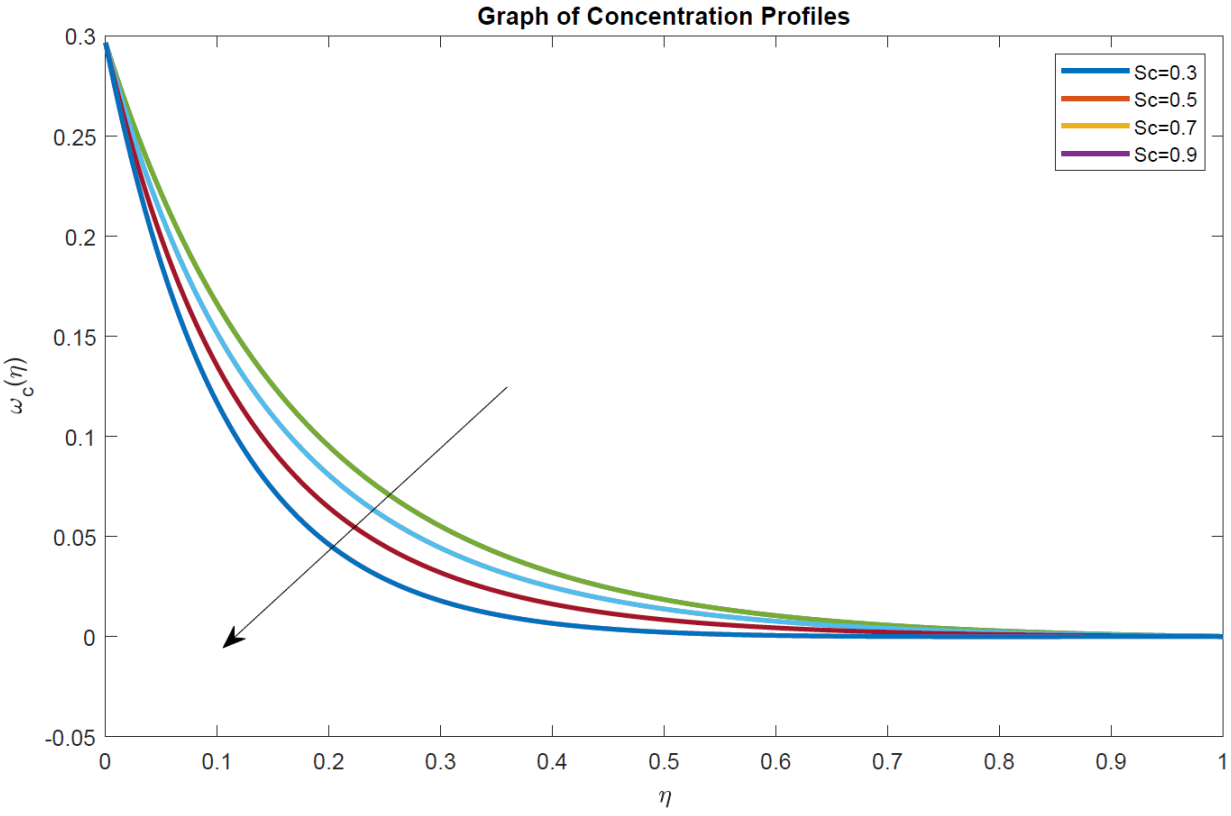

Figure 17. *Concentration profiles for different values of Sc.*

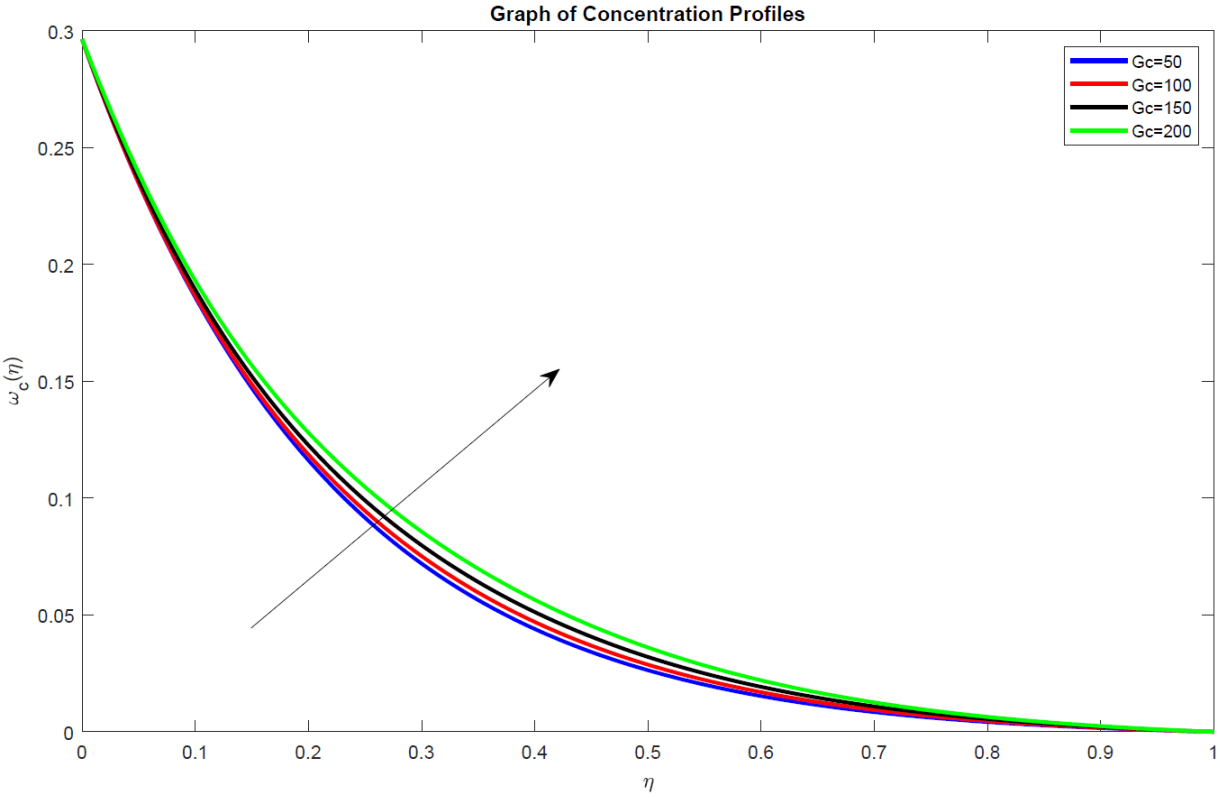

Figure 18. *Concentration profiles for different values of Gc.*

5.4. Effects of Variation of Parameters on Skin Friction

From table 1, It is noted that increase in the values of Reynolds number, skin friction decreases. This due to the reason that skin friction depend on the viscous forces of the fluid. So the higher the Reynolds number tend to reduce the viscous force hence skin friction reduce. it has been observed that increase in Eckert number and Pradit number there is an increase in skin friction. Also the thermal and concentration Grashof number, Hartman number and unsteadiness parameter increases skin friction as they increase. Furthermore, An increase in the Soret number and Dufour number results in increased skin friction.

The table 1 below show the results of Skin friction for various values of physical parameters.

Table 1. *Skin friction coefficient for various values of dimensionless numbers.*

Pr	Ec	Sc	Sr	Re	Γ	λ	Gr	Gc	Du	Ha	Cf
0.71	0.22	0.2	1	3	0.1	0.1	1	1	1	1	0.5219096
2	0.22	0.2	1	3	0.1	0.1	1	1	1	1	0.5247935
0.71	5	0.2	1	3	0.1	0.1	1	1	1	1	0.5267075
0.71	0.22	1.5	1	3	0.1	0.1	1	1	1	1	0.5230474
0.71	0.22	0.2	2	3	0.1	0.1	1	1	1	1	0.52188582
0.71	0.22	0.2	1	5	0.1	0.1	1	1	1	1	0.3101531
0.71	0.22	0.2	1	3	1.5	0.1	1	1	1	1	0.5218948
0.71	0.22	0.2	1	3	0.1	1	1	1	1	1	0.4629746
0.71	0.22	0.2	1	3	0.1	0.1	10	1	1	1	0.5797684
0.71	0.22	0.2	1	3	0.1	0.1	1	10	1	1	0.5763336
0.71	0.22	0.2	1	3	0.1	0.1	1	1	2	1	0.5762769
0.71	0.22	0.2	1	3	0.1	0.1	1	1	0.1	1.2	0.5832763

5.5. Effects of Variation of Parameters on Rate Heat Transfer

The following are the observable effects of different parameters on Nusselt number as shown in Table 2. Rise in Prandtl number results to an increase in the Nusselt number. A low Prandtl number indicates that heat conduction is more influential than convection. When the Prandtl number is

high, convection is more effective than pure conduction in transferring energy from an area, so momentum diffusivity is dominant. The Nusselt number increases with rise in the Eckert number, Reynolds, Dufour number, Reynolds parameter, unsteadiness parameter and Hartmann number. There is little or no change in the Nusselt number when the Schmidt number, Soret number, chemical reaction parameter and concentration Grashof number are altered. However, the Nusselt number slightly decreases when the thermal Grashof number increased.

Table 2. *Nusselt number for various values of dimensionless numbers.*

Pr	Ec	Sc	Sr	Re	Γ	λ	Gr	Gc	Du	Ha	Nu
0.71	0.22	0.2	1	3	0.1	0.1	1	1	1	1	-0.9775911
3	0.22	0.2	1	3	0.1	0.1	1	1	1	1	-1.0027663
0.71	5	0.2	1	3	0.1	0.1	1	1	1	1	-1.0164227
0.71	0.22	1.5	1	3	0.1	0.1	1	1	1	1	-0.9731386
0.71	0.22	0.2	2	3	0.1	0.1	1	1	1	1	-0.9780804
0.71	0.22	0.2	1	5	0.1	0.1	1	1	1	1	-0.9795281
0.71	0.22	0.2	1	3	1.5	0.1	1	1	1	1	-0.9777634
0.71	0.22	0.2	1	3	0.1	1	1	1	1	1	-0.9795529
0.71	0.22	0.2	1	3	0.1	0.1	10	1	1	1	-0.9778123
0.71	0.22	0.2	1	3	0.1	0.1	1	10	1	1	-0.9779078
0.71	0.22	0.2	1	3	0.1	0.1	1	1	2	1	-0.9783239
0.71	0.22	0.2	1	3	0.1	0.1	1	1	0.1	1.2	-0.9778536

5.6. Effects of Variation of Parameters on Mass Transfer Rate

It has been depicted in Table 3 that when there is increase in chemical reaction number, dufour parameter and prandtl number, the Sherwood number is reduced. On the other side, the Sherwood number is increased when the Eckert, Schmit, or Soret numbers are raised. However, there is little or no effect of the Reynolds number, unsteadiness parameter, Grashof numbers, or Hartmann number on the Sherwood number.

Table 3. *Sherwood number for various values of dimensionless numbers.*

Pr	Ec	Sc	Sr	Re	Γ	λ	Gr	Gc	Du	Ha	Sh
0.71	0.22	0.2	1	3	0.1	0.1	1	1	1	1	-0.9743499
2	0.22	0.2	1	3	0.1	0.1	1	1	1	1	-0.9723692
0.71	5	0.2	1	3	0.1	0.1	1	1	1	1	-0.9809951
0.71	0.22	1.5	1	3	0.1	0.1	1	1	1	1	-1.008994
0.71	0.22	0.2	2	3	0.1	0.1	1	1	1	1	-0.9736637
0.71	0.22	0.2	1	5	0.1	0.1	1	1	1	1	-0.9744119
0.71	0.22	0.2	1	3	1.5	0.1	1	1	1	1	-0.9741096
0.71	0.22	0.2	1	3	0.1	1	1	1	1	1	-0.9745738
0.71	0.22	0.2	1	3	0.1	0.1	10	1	1	1	-0.9743552
0.71	0.22	0.2	1	3	0.1	0.1	1	10	1	1	-0.9743596
0.71	0.22	0.2	1	3	0.1	0.1	1	1	3	1	-0.9740929
0.71	0.22	0.2	1	3	0.1	0.1	1	1	0.1	1.2	-0.9743472

5.7. Validation

Comparison with previous studies available in the literature has been done and an excellent agreement established. These results agrees with [27] when there is absence of dufour effect. The findings were When Eckert number (Ec) was increased the temperature and velocity profiles increased. Also When magnetic parameter (Ha) increase, velocity profile decrease while temperature raised and when Soret number (Sr) increased it reduces concentration profiles.

6. Conclusions

This study has investigate soret and dufour effects on unsteady Newtonian MHD fluid with mass and heat transfer in a Collapsible tube by using Spectral Based Collocation Method. This paper has developed model of the mathematical equations governing the fluid flow in a cylindrical collapsible elastic tube. This equations were non-linear partial differential equations which later were converted to non-linear ordinary differential equations and solved using bvp4c in MATLAB.

The results have shown that the equations can be used to predict MHD fluid flow through a collabsible elastic tube for different behaviors. The obtained model is significant for the field as it provide framework for understanding and predicting MHD flow in similar systems. However this model of mathematical equations are based on a certain assumptions and limitations. Also this study has determined the velocity, concentration, and temperature profiles of the fluid flow through a cylindrical collapsible tube. The effect of varying various flow parameters on the velocity, concentration and temperature distributions have been determined and the results are presented graphically and it leads to conclusion that:

1. The fluid velocity increase with increase in Reynolds number (Re), thermal Grashof number (Gr), Soret number (Sr), while decrease with increase in Hartman number (Ha).
2. The temperature of the fluid increases with increase Reynolds number (Re), Eckert number (Ec), Hartman number (Ha), Schmidt number (Sc) while decrease with increase in Dufour number (Du) and Soret number (Sr).
3. The concentration of the fluid decrease with increase in Dufour number (Du), chemical reaction parameter (Γ), Eckert number (Ec) whereas increase with an increase in Soret number (Sr)
4. The rate of heat transfer increase with an increase in Eckert number (Ec), Prandtl number (Pr), Hartman number (Ha), Unsteadiness parameter (λ). There is a little or no change in the Nusselt number (Nu) with change in Soret number (Sr), Schmidt number (Sc), Reynolds number (Re), chemical reaction parameter (Γ) and concentration Grashof number (Gc).
5. The Mass transfer rate decrease with increase in Prandtl number (Pr), chemical reaction parameter (Γ) while increase with increase Eckert number (Ec), Schmidt number (Sc) and Soret number (Sr). However no effective change in Hartman number Ha, thermal Grashof number (Gr), Reynolds number (Re) and Unsteadiness parameter (λ)

The results obtained from this study can be used in medicine where by the skin-friction coefficient is very important since it enables regulation of blood pressure, preventing of blood clots which may cause a serious health issue i.e stroke. Hence addressing skin friction-related issues is essential in preventing and managing cardiovascular diseases. Also it can be used in thermotherapy, where controlled heat is used to treat injuries or conditions like muscle pain, arthritis.

Future work can be conducted on steady, three-dimensional, MHD fluid flow of mass and heat transfer through collapsible tubes with varying magnetic field for laminar flow.

Nomenclature

u_z	Vertical velocity, meters (ms^{-1})	m	Arbitrary constant
u_θ	Angular velocity, rad ($rad\ s^{-1}$)	I	Electric current, Ampere (A)
u_r	Radial velocity, meters (ms^{-1})	J	Electric current density, (Am^{-2})
u	Speed of the fluid, (ms^{-1}).	$\overrightarrow{q}$	Velocity vector
c	Speed of light, meters (ms^{-1})	$\overrightarrow{E}$	Electric current vector
$c(z)$	Constant function of z	$\overrightarrow{F_i}$	Body forces, (Nm)
r	Radius of the tube, meters (m)	F_g	Force due to gravity
a_0	Characteristic radius, meters (m)	$\overrightarrow{F_L}$	Lorentz Force
z	Axial coordinate, meters (m)	$\overrightarrow{B}$	Magnetic vector
t	Time, seconds (s)	∇	Vector differential operator
B_0	Constant magnetic field, Tesla (T)	∇^2	Laplacian operator
K_t	Thermal diffusion ratio	R	Rate of chemical reaction
T	Temperature, kelvin (K)	g	Gravitational constant, (Nm^2kg^{-2})
T_0	Temperature at the center, kelvin (K)	q_h	Heat flux, (Wm^{-2})
T_w	Temperature at the wall, kelvin (K)	q_m	Mass flux, ($kg\ m^{-2}s^{-1}$)
T_m	Mean temperature, kelvin (K)	Re	Reynolds number
C	Concentration, mole per cubic meter mol/m^3	Pr	Prandtl number
C_0	Concentration at the center, mole per cubic meter mol/m^3	Ec	Eckert number
C_w	Concentration at the wall, mole per cubic meter mol/m^3	Ha	Hartmann number
C_s	Concentration Susceptibility	Gr	Thermal Grashof number
C_p	Specific heat capacity, ($J\ kg^{-1}\ K^{-1}$)	Gc	Concentration Grashof number
D_m	Concentration diffusion parameter, (m^2s^{-1})	Sc	Schmidt number
k_r	Chemical reaction coefficient, (Ms^{-1})	Sr	Soret number
Q	Discharge, (m^3s^{-1})	Du	Dufour parameter
$f(\eta)$	Dimensionless velocity	C_f	Skin friction coefficient
P	Pressure, (Nm^{-2})	Nu	Nusselt number
V	Volume, (m^3)	Sh	Sherwood number

Acknowledgments

The authors are grateful to the Pan African University Institute for Basic Sciences, Innovation and Technology (PAUSTI) and Taita Taveta University for their supportive environment throughout the conduct of the study.

Conflicts of Interest

The authors declare that they have no confcts of interest.

References

[1] O. Makinde, "Collapsible tube flow: A mathematical model," 2005.

[2] X. Luo, Z. Cai, W. Li, and T. Pedley, "The cascade structure of linear instability in collapsible channel flows," Journal of Fluid Mechanics, vol. 600, pp. 45-76, 2008.

[3] P. Lakshmi Narayana and P. Murthy, "Soret and dufour effects on free convection heat and mass transfer from a horizontal flat plate in a darcy porous medium," 2008.

[4] S. Odejide, Y. Aregbesola, and O. Makinde, "Fluid flow and heat transfer in a collapsible tube," Romanian Journal of Physics, vol. 53, pp. 499-506, 2008.

[5] C.-Y. Cheng, "Soret and dufour effects on natural convection heat and mass transfer from a vertical cone in a porous medium," International Communications in Heat and Mass Transfer, vol. 36, no. 10, pp. 1020-1024, 2009.

[6] E. Marchandise and P. Flaud, "Accurate modelling of unsteady flows in collapsible tubes," Computer Methods in Biomechanics and Biomedical Engineering, vol. 13, no. 2, pp. 279-290, 2010.

[7] S. El-Kabeir, "Soret and dufour effects on heat and mass transfer due to a stretching cylinder saturated porous medium with chemically-reactive species," Latin American applied research, vol. 41, no. 4, pp. 331-337, 2011.

[8] D. Pal and H. Mondal, "Influence of chemical reaction and thermal radiation on mixed convection heat and mass transfer over a stretching sheet in darcian porous medium with soret and dufour effects," Energy Conversion and Management, vol. 62, pp. 102-108, 2012.

[9] D. Pal and S. Chatterjee, "Soret and dufour effects on mhd convective heat and mass transfer of a powerlaw fluid over an inclined plate with variable thermal conductivity in a porous medium," Applied Mathematics and Computation, vol. 219, no. 14, pp. 7556-7574, 2013.

[10] A. Siviglia and M. Toffolon, "Multiple states for flow through a collapsible tube with discontinuities," Journal of fluid mechanics, vol. 761, pp. 105-122, 2014.

[11] C. W. Kanyiri, M. Kinyanjui, and K. Giterere, "Analysis of flow parameters of a newtonian fluid through a cylindrical collapsible tube," SpringerPlus, vol. 3, no. 1, pp. 1-12, 2014.

[12] M. S. Ullah, A. Tarammim, and M. J. Uddin, "A study of two dimensional unsteady mhd free convection flow over a vertical plate in the presence of radiation," Open Journal of Fluid Dynamics, vol. 11, no. 1, pp. 20-33, 2021.

[13] V. Kaigalula, J. Okelo, S. Mutua, and O. Muvengei, "Magneto-hydrodynamic flow of an incompressible fluid in a collapsible elastic tube with mass and heat transfer," Journal of Applied Mathematics and Physics, vol. 11, no. 11, pp. 3287-3314, 2023.

[14] I. J. U. Uwem Ekwere Inyang, "Heat transfer in helical coil heat exchanger," Advances in Chemical Engineering and Science, vol. 12, no. 1, pp. 29-39, 2022.

[15] S. Odejide, "Fluid flow and heat transfer in a collapsible tube with heat source or sink," Journal of the Nigerian Mathematical Society, vol. 34, no. 1, pp. 40-49, 2015.

[16] K. J. Mwangi, Unsteady magnetohydrodynamic fluid flow in a collapsible tube. PhD thesis, Appled Mathematics, JKUAT, 2016.

[17] V. Anand and I. C. Christov, "Steady low reynolds number flow of a generalized newtonian fluid through a slender elastic tube," arXiv preprint arXiv: 1810.05155, pp. 62-72, 2018.

[18] A. Mehdari, M. Agouzoul, and M. Hasnaoui, "Analytical modelling for newtonian fluid flow through an elastic tube," 2018.

[19] P. Maurice, K. Giterere, and R. Kiongora, "Unsteady flow of a newtonian fluid through a cylindrical collapsible tube," 2019.

[20] D. Chepkonga, R. Kiogora, and K. Giterere, "Fluid flow and heat transfer through a vertical cylindrical collapsible tube in the presence of magnetic field and an obstacle," International Journal of Advances in Applied Mathematics and Mechanics, pp. 2347-2529, 01 2019.

[21] R. D. Alsemiry, P. K. Mandal, H. M. Sayed, N. Amin, et al., "Numerical solution of blood flow and mass transport in an elastic tube with multiple stenoses," BioMed research international, vol. 2020, 2020.

[22] A. Idowu and B. Falodun, "Effects of thermophoresis, soret-dufour on heat and mass transfer flow of magnetohydrodynamics non-newtonian nanofluid over an inclined plate," Arab Journal of Basic and Applied Sciences, vol. 27, no. 1, pp. 149-165, 2020.

[23] S. Priyadharsini, "Unsteady flow of collapsible tube under transverse magneto hydrodynamic fluid," International Journal of Advanced Science and Technology, vol. 29, pp. 1995-2001, Jan. 2020.

[24] X. Ou, R. Wang, T. Guo, C. Shao, and Z. Zhu, "Numerical investigation on the heat and mass transfer in microchannel with discrete heat sources considering the soret and dufour effects," Micromachines, vol. 13, no. 11, p. 1848, 2022.

[25] S. M. Moghimi et al., "Heat transfer of mhd flow over a wedge with surface of mutable temperature," Authorea Preprints, 2023.

[26] F. Hussain, M. Nazeer, A. Mengal, A. Hussain, and S. A. R. Shah, "Numerical simulation of mhd twodimensional flow incorporated with joule heating and nonlinear thermal radiation," ZAMM-Journal of Applied Mathematics and Mechanics/Zeitschrift f¡§ur Angewandte Mathematik und Mechanik, p. e202100246, 2023.

[27] N. Mwamba, J. Okelo Abonyo, K. O. Awuor, et al., "Effects of thermal radiation and chemical reaction on hydromagnetic fluid flow in a cylindrical collapsible tube with an obstacle," International Journal of Mathematics and Mathematical Sciences, vol. 2023, 2023.

[28] V. Ojiambo, M. Kinyanjui, and M. Kimathi, "A study of two-phase jeffery hamel flow in a geothermal pipe", 2018.

[29] N. C. Wawira, M. Kinyanjui, K. Giterere, et al., "Hydromagnetic non-newtonian fluid flow in a convergent conduit," Journal of Applied Mathematics, vol. 2022, 2022.

[30] L. N. Trefethen, "Spectral methods in matlab, volume 10 of software, environments, and tools," Society for Industrial and Applied Mathematics (SIAM), Philadelphia, PA, vol. 24, p. 57, 2000.